DECLASSIFIED

~~RESTRICTED~~ UNCLASSIFIED

NRL REPORT R-3422

FR-3420

INVESTIGATION AND ANALYSIS OF "CAPTURE EFFECT" IN F-M AND A-M COMMUNICATION SYSTEMS

DECLASSIFIED by NRL Contract
Declassification Team
Date: 6 JAN 2017
Reviewer's name: [redacted]

Declassification authority: NAVY DECLASS GUIDE/NAVY DECLASS MANUAL 11 DEC 2012
06 SERIES

DISTRIBUTION STATEMENT A APPLIES.
Further distribution authorized by UNLIMITED only.

NAVAL RESEARCH LABORATORY

WASHINGTON, D.C.

~~RESTRICTED~~ UNCLASSIFIED DECLASSIFIED

DECLASSIFIED

3460

RESTRICTED

NRL REPORT R-3422

UNCLASSIFIED

INVESTIGATION AND ANALYSIS OF "CAPTURE EFFECT" IN F-M AND A-M COMMUNICATION SYSTEMS

DEPARTMENT OF THE NAVY ★ OFFICE OF NAVAL RESEARCH ★

NAVAL RESEARCH LABORATORY

WASHINGTON, D.C.

RESTRICTED

DECLASSIFIED

DECLASSIFIED

RESTRICTED

SECURITY

Reproduction of this classified document in any form or the making of extracts therefrom by other than naval activities is not authorized except by specific approval of the Secretary of the Navy.

It is forbidden naval activities to make extracts from or to copy this classified document without specific approval of the Chief of Naval Operations or originator, as applicable, except as provided for in articles 9-9 and 9-10 of the United States Navy Security Manual for Classified Matter.

This document contains information affecting the national defense of the United States within the meaning of the Espionage Act, 50 U.S.C., 31 and 32, as amended. Its transmission or the revelation of its contents, in any manner to an unauthorized person, is prohibited by law.

DECLASSIFIED

RESTRICTED

DECLASSIFIED

RESTRICTED

NRL REPORT R-3422

UNCLASSIFIED

INVESTIGATION AND ANALYSIS OF "CAPTURE EFFECT" IN F-M AND A-M COMMUNICATION SYSTEMS

R. W. Zeek

February 18, 1949

Approved by:

Mr. T. McL. Davis, Head, Radio Techniques Branch
Mr. L. A. Gebhard, Superintendent, Radio Division II

NAVAL RESEARCH LABORATORY
CAPTAIN F. R. FURTH, USN, DIRECTOR
WASHINGTON, D.C.

RESTRICTED

DECLASSIFIED

DISTRIBUTION

BuShips	
Attn: Code 910B and 926	(20)
CNO	
Attn: Code OP-413-B2	(5)
BuAer	
Attn: Code EL-4	(1)
Attn: Code EL-92	(1)
Attn: Code TD-4	(1)
ONR	
Attn: Code 482	(2)
CO, ONR, Boston	(1)
ComOpDevFor	(1)
Dir., USNEL	(2)
Cdr., USNOTS	
Attn: Reports Unit	(2)
SNLO, USNELO	(1)
Ch. of Staff, USAF	(1)
OCSigO	
Attn: Ch. Eng. & Tech. Div., SIGTM-S	(1)
CO, SCEL	
Attn: Dir. of Engineering	(2)
BAGR, CD, Wright-Patterson Air Force Base	
Attn: BAU-ADD	(1)
CG, AMC, Wright-Patterson Air Force Base	
Attn: Eng. Div., Electronics Subdiv., MCREEO-2	(1)
CO, 4151st Air Force Base Unit, Red Bank	
Attn: Ch. Eng. Div., WLENG	(1)
CO, 4153rd Air Force Base Unit, Cambridge	
Attn: ERCTL	(1)
RDB	
Attn: Library	(2)
Attn: Navy Secretary	(1)
Science and Technology Project	
Attn: Mr. J. H. Heald	(2)

UNCLASSIFIED

CONTENTS

ABSTRACT

"Capture effect" is a phenomenon occurring in both a-m and f-m communication systems manifest in the depression of a relatively weak desired signal by a stronger interfering signal at or near the desired-signal frequency, the degree of depression depending on circuit design, absolute and relative input amplitudes of the two signals, and on their frequency location relative to predetector selectivity. An analysis is presented which considers how and in what circuits of a receiving system the effect occurs and the degree of capture to be encountered under various conditions of receiver circuitry. Control or reduction of the effect is discussed.

Limiters, discriminators, detectors, thermionic-bias potentials, AVC systems, detuning, de-emphasis networks, AFC systems, noise-peak limiters, and fluctuation- and impulse-noise are treated with regard to their influence on the over-all capture effect. Theoretical analysis is supported by experimental data wherever practicable.

It is found that difference in degree of capture between a-m and f-m systems is due to action of limiter and discriminator circuits in FM and that the nearer any circuit approaches the "ideal," the greater the degree of capture experienced. In a-m systems capture may be reduced by (1) use of square-law rectifiers as final detectors and/or (2) operation without AVC; in f-m systems reduction is accomplished by (1) use of square-law rectifiers following the discriminator element, (2) increase in discriminator bandwidth, (3) reduction in effectiveness of limiting, and/or (4) incorporation of discriminators with nonsymmetrical and/or nonlinear characteristics.

PROBLEM STATUS

This report, together with a forthcoming NRL Report R-3460 "An investigation of Nonlinear Circuits Under Two-Signal Conditions," Restricted, by W. E. W. Howe, concludes work on this problem. Unless otherwise notified by the Bureau of Ships, the Laboratory will consider this problem closed one month from the mailing date of the latter report.

AUTHORIZATION

NRL Problem No. R01-19R

INVESTIGATION AND ANALYSIS OF "CAPTURE EFFECT" IN F-M AND A-M COMMUNICATION SYSTEMS

INTRODUCTION

"Capture" is the term commonly applied to a desired-signal output depression effect which occurs in frequency-modulated reception. The effect is present in amplitude-modulated reception also but usually to a more limited degree than in frequency modulation. It is generally present whenever an interfering signal stronger than the desired signal is tuned to or near the desired-signal frequency. The phenomenon manifests itself as a depression of the weaker signal's output by the stronger one, the degree of depression depending on the design of the receiver circuits, the absolute and relative input amplitudes of the two signals, and on their location in frequency relative to the predetector selectivity of the receiver.

This investigation of capture effect has been conducted to determine in what stages, circuits, or elements of the receiving system capture occurs, and to what degree. Both theoretical and experimental consideration have been given to such items as amplifier-, detector-, and AVC action in a-m reception and limiter-, discriminator-, and detector action in f-m reception. For the purposes of this report, the term "discriminator" refers to the means for converting frequency variations into amplitude variations for subsequent detection purposes. The term "f-m detector" refers to the necessary combination of the discriminator and rectifier circuits and elements.

The terms "capture" and "capture threshold" have been used rather freely in much of the technical literature relating to this phenomenon. In speaking of capture, the words "suppression" and "elimination" are frequently encountered and interchangeably used. For purposes of discussion of the effect in this report, the following definitions have been devised.

(1) Capture - the suppression of the desired-signal output caused by the presence of an undesired carrier at or near the desired-signal carrier frequency.

(2) Capture Threshold - the undesired-to-desired input carrier level ratio at which the desired-signal output is depressed 3 db below its interference-free value. This usually occurs in the vicinity of undesired-to-desired-signal input carrier level ratios of 1.

(3) Standard Depression Capture Ratio - the undesired-to-desired input carrier level ratio at which the desired-signal output has been depressed to such a degree as essentially to prevent transfer of intelligence. A depression or attenuation of the desired-signal output of about 30 db is suggested as a satisfactory standard. This agrees fairly well with telephone cross-talk standards. Unless otherwise stated, a 30-db depression will be used in this report for designation of Standard Depression Capture Ratio.

(4) Complete Capture Level - the desired-signal output level at which the desired signal is apparently eliminated completely from the output of the receiver. This would normally correspond to a depression of desired-signal output of at least 40 db.

The original directive[1*] under which this investigation has been conducted was a request "to investigate and determine the practicability of f-m receiver circuits designed to eliminate or minimize the capture effects of strong jamming carriers, modulated and unmodulated, on f-m signals." The directive made no mention of capture effect in a-m reception, but since a-m and f-m receiver circuitry are closely related, and since the ultimate goal as stated in the problem was to "evaluate the relative merits of a-m and f-m communication systems," it was considered highly desirable and entirely within the scope of this problem to investigate capture effect in a-m reception as well.

It was also stated in the original directive that "capture has proved to be a strong disadvantage, from a military standpoint, for f-m." Definite information was requested as to whether the capture effect can be minimized. Two references were given[2,3] which supposedly contain suggestions for the reduction of this effect. NRL has, as yet, been unable to obtain the first of these references[2] for investigation and analysis. The second[3] suggests a "back-bias" scheme for minimizing capture which, in effect, changes the threshold of limiting. This system will be mentioned again later.

There are several other co-channel and adjacent-channel effects which can cause the desired signal to be suppressed or completely jammed. For instance, there is the presence of audible beat notes and/or cross-modulation products in the output which can make the transfer of intelligence by the desired signal difficult or impossible to achieve. These effects are sometimes confused with the capture effect, and in fact several writers have used the term "capture" to include any or all of the interference products appearing in the output of a receiver. These interference products would better be termed "co-channel" or "adjacent channel" interference effects, of which capture is one term. This report will be confined mainly to the capture effect proper. Accompanying heterodyne and other effects can, however exceed capture in importance under some circumstances. Many of these other two-signal effects have been investigated as part of the problem and are discussed in a forthcoming companion report.[4]

In any analysis of capture phenomenon, consideration must first be given to study of the particular circuits or stages of the receiving system in which the effect can occur. In an a-m receiver, the effect is localized mainly in the detector circuits and the AVC system, with predetector amplifier saturation also appearing as a factor in the absence of effective AVC. In an f-m receiver, the effect involves both the detector rectifiers and the limiter circuits, as well as the discriminator (slope-filter) element which is not usually present in the a-m system. It is generally possible to predict with reasonable accuracy the degree of capture possible in either an a-m or f-m system, provided the following receiver conditions are known:

(1) Final Detector Rectifiers

A. Mode of rectifier operation

(a) Linear-Law

(b) Square-Law

(c) Intermediate

---

*See page 55 for references.

B. Rectifier type

(a) Single-ended

(b) Balanced (symmetry known)

(c) Crystal or Thermionic Diodes

(2) Limiters

A. Type

(a) Grid-bias plate-saturation amplifier

(b) Shunt-diode (full or half-wave)

(c) Others (such as series-diode, etc.)

B. Operating conditions

(a) Threshold level (onset of limiting)

(b) Normal operation (well above threshold but below blocking level)

(c) Blocking level

C. Time constants

D. Loading effect of noise-limiter in a-m system

E. Presence and effectiveness of automatic-frequency-control (AFC) system

(3) Discriminator

A. Type

(a) Single-slope filter (such as frequency-counter type)

(b) Dual-slope filters (such as phase-discriminator type)

B. Frequency-amplitude characteristic

(a) Linear

(b) Nonlinear

(c) Symmetrical

(d) Nonsymmetrical

C. Centering

(a) Desired input signal centered

(b) Desired input signal off-center

D. Bandwidth

E. Deviation (Modulation)

(a) Deviation within discriminator band-limits

(b) Deviation exceeding discriminator band-limits.

It must be emphasized that the difference in degree of capture to be found between the a-m and f-m systems is primarily a function of the effectiveness of the circuits provided for operation with the type of modulation employed. The f-m receiver differs from the a-m receiver mainly in that it requires additional elements for conversion of the intelligence-carrying modulation from variations in frequency to variations in amplitude for detection purposes. The necessary additional elements, consisting of a discriminator (slope filters) and one or more predetection amplitude limiters, account for the major differences in the degree of capture obtained between the two modulation types. Variations in limiting and/or detector characteristics between two similar receivers can also cause considerable variation in the relative degree of capture. This will be discussed later in greater detail.

THEORETICAL TREATMENT OF PROBLEM

The following analysis treats those elements or circuits of a receiving system which contribute to capture, together with a discussion of their combination into the over-all capture effect.

Amplitude Detectors

The apparent demodulation of a weaker signal by a stronger one in an a-m detector with a linear-law detection characteristic is a well known effect. Many writers have mentioned this phenomenon, and several analyses of it have been given in technical literature.[5,6,7,8,9,10] The analysis of E. V. Appleton and D. Boohariwalla[6] is one of the better-known theoretical treatments of this effect. The complete derivation, with certain changes in nomenclature and clarifying statements added, will be found in Appendix A; the results, briefly, are as follows.

If a desired carrier of amplitude D_i and an undesired carrier, U_i, (differing in frequency by a value outside the pass-band of the detector output circuits) appear in the same channel (within the predetector pass-band of the receiver) and are demodulated in a linear-law rectifier, the modulation output, D_o, from the desired carrier is reduced by a value proportional to the ratio of D_i to U_i. Thus,

$$D_o = \frac{D_i}{2\,U_i}, \tag{1}$$

provided that U_i is stronger than D_i by at least a factor of 2, or

$$U_i \cong 2\,D_i$$

where D_i is the input amplitude of the desired carrier (modulated), U_i is the input amplitude of the undesired carrier (unmodulated), and D_o is the output resulting from the desired modulated carrier in the presence of the undesired carrier.

In a similar manner, the effect of a weak undesired signal, U_i, on a stronger desired signal, D_i, is found to be

$$D_o' = 1 - 1/4\left(\frac{U_i}{D_i}\right)^2, \tag{2}$$

provided that D_i is stronger than U_i by at least a factor of 2, or

$$D_i \cong 2\,U_i$$

where D_o' is the output resulting from the desired modulated carrier in the presence of the undesired carrier.

Equation (1) shows that the depression of the desired-signal output by a stronger undesired carrier is quite pronounced, whereas equation (2) shows that the depression of the desired-signal output by a weaker undesired carrier is slight. It should be noted that these signal depressions or capture effects may be obscured by heterodyne beats between D and U signals, unless the beats are filtered out or are outside the pass-band of the detector output system.

A more general treatment of the detector capture phenomenon will be found in Appendix B, in which (unlike the treatment in reference 9) the modulation factor is included in the first mathematical statement of the problem. This treatment has been carried out for the square-law detector as well as for the linear-law detector. The results in the linear case are in agreement with those given in equation (3A) of the Appleton-Boohariwalla treatment (Appendix A). The results in the square-law case are in agreement with statements to be found scattered throughout the technical literature, although this writer has not previously encountered a mathematical treatment giving the output-level equations of the square-law detector in the presence of two signals. The square-law case will be discussed again later.

A graph of equations (1) and (2) is shown as curve (A) in Figure 1, presented in the general form used throughout to illustrate capture. It is evident from this curve that, with ideal linear-law detection, the depression of the desired signal is 1 db per db of increase in level of the undesired carrier whenever the undesired carrier exceeds the amplitude of the desired by approximately 3 db or more. Variation to this extent represents a "capture-slope" of 45°. The discontinuity of curve (A) in the region of signal equality (dashed portion between U/D = ± 2 db) probably is caused by the failure of certain

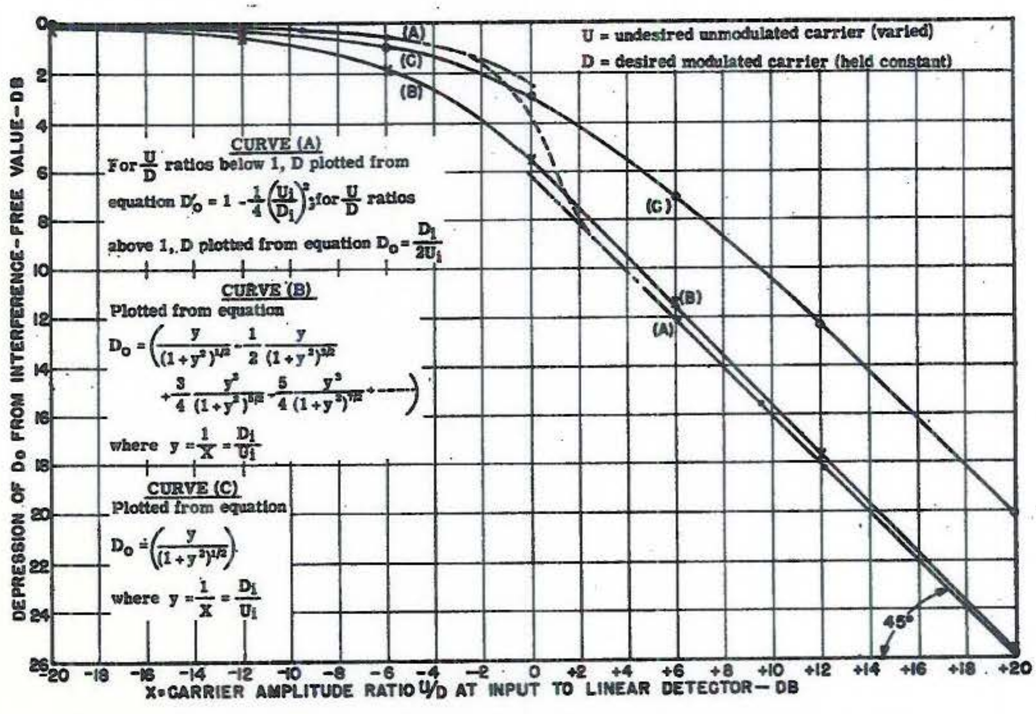

Fig. 1 - Depression of a constant desired signal by an undesired signal of varying value in the output of a linear-law detector

simplifying assumptions made in the derivation of equations (1) and (2). Curve (B) of Figure 1, however, has been plotted from equation (3A) of Appendix A, which represents a more exact solution carried out to 4 terms. The capture slope as shown by curve (B) is still about 45°, but the absolute depression of the desired signal (in the region where the ratio U/D > 0 db) is slightly less than for curve (A), and the curve exhibits no discontinuities at the threshold. The depression of D at the threshold as shown by this curve is approximately 5.5 db.

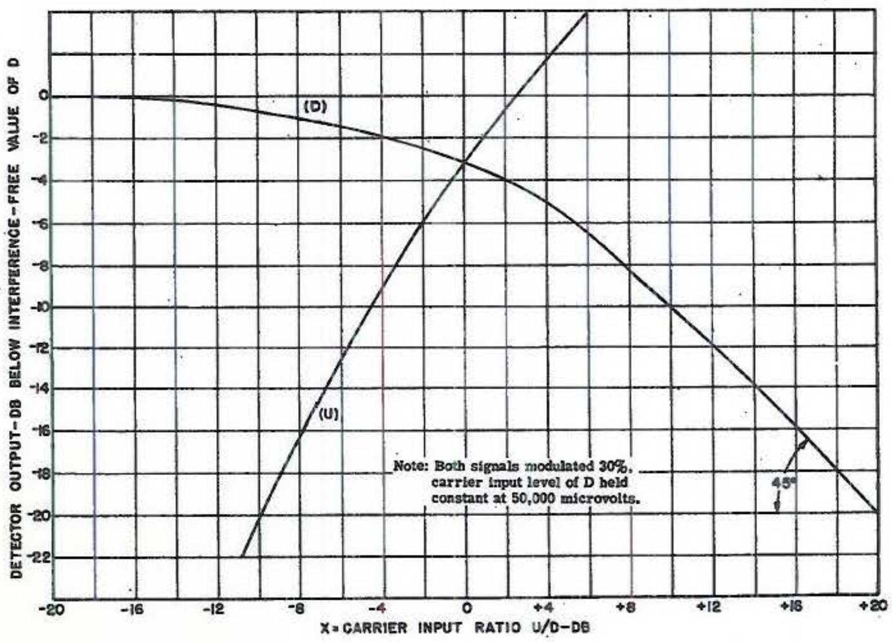

Fig. 2 - Measured capture effect in a-m detector at high input levels (linear-law rectification)

Experimental curves of the capture effect occurring with a linear-law detector appear in the companion report[4] and are shown replotted in Figure 2 of this report. The measurements were made by feeding two signals of slightly different modulation and carrier frequencies into an r-f amplifier and linear a-m detector and filtering the desired modulation tone from the detector output with a wave-analyzer. The resulting curves have a slope of about 45° in the region where U/D > 6 db, but the depression of D at the threshold (U/D = 0 db) is only 3 db. The over-all depression or capture is then approximately 6 db less than that exhibited in curve (B) of Figure 1 in the region where U/D > 6 db. This result is in very close agreement with the first term in equation (3A) of Appendix A, i.e.,

$$D_o = \left(\frac{y}{(1 + y^2)^{1/2}}\right) \tag{3}$$

where

$$y = \frac{1}{x} = \frac{D_i}{U_i}.$$

Curve (C) of Figure 1 shows a plot of the above term (equation 3) which, as can be seen in Figure 2, is in almost exact agreement with the experimental results. The difference between curves (A) and (B) of Figure 1 compared to curve (C) is not one of slope (each about 45°) but rather one of depression at the threshold and above. This discrepancy will bear further examination in some subsequent investigation but it will not be pursued further in this report. It should be noted, however, that some doubt is cast as to the absolute attenuation of the desired-signal output at the threshold and beyond.

The theoretical equations for capture in a linear a-m detector do not consider the "contact" or internal thermionic potential developed in the usual diode tube used as detector. In crystal diodes, the internal thermal potential is generally negligible, but in the thermionic type of diode tube usually employed as a detector the internal potential developed is considerable. It is in the region of 1.2 volts for a type 6H6, for example. This potential makes the absolute amplitudes of the input signals U and D at the detector or other nonlinear element important with respect to the degree of capture obtained. If the input carriers are of such level that the resultant composite mean signal exceeds the thermionic-bias voltage, a given depression of the desired signal will occur at a lower ratio of U/D. However, if the input carriers are weak, so that the resultant composite input-signal amplitude is below the value of diode bias, the threshold of capture would be higher in terms of U/D ratio than that shown by curve (C) of Figure 1. The desired-signal output in this case is shown in Figure 3 of this report, where the capture curve exhibits 1/2-db depression of D at U/D = 0 db and generally less capture over-all (slope $< 45°$) for the low-input level values of the carriers employed. Further experimental verification will be found in the companion report.[4] The transition between square-law and linear-law detector operation, as indicated by this experimental curve, is gradual. In effect, the thermionic-bias potential constrains the weak input carriers to operate on a region of the detector characteristic which is intermediate between square-law and linear-law. With a perfect or ideal square-law detector, the output is proportional to the square of the input-signal voltage. This logarithmic characteristic is in opposition to the linear-law capture effect described above and results in a theoretical capture slope of zero degrees for all input-carrier ratios (U/D). Thus such a detector would exhibit no capture characteristics of its own. This is verified by equation (1B) of Appendix B, where the modulation output due to the D signal is seen to be independent of the interfering carrier, U.

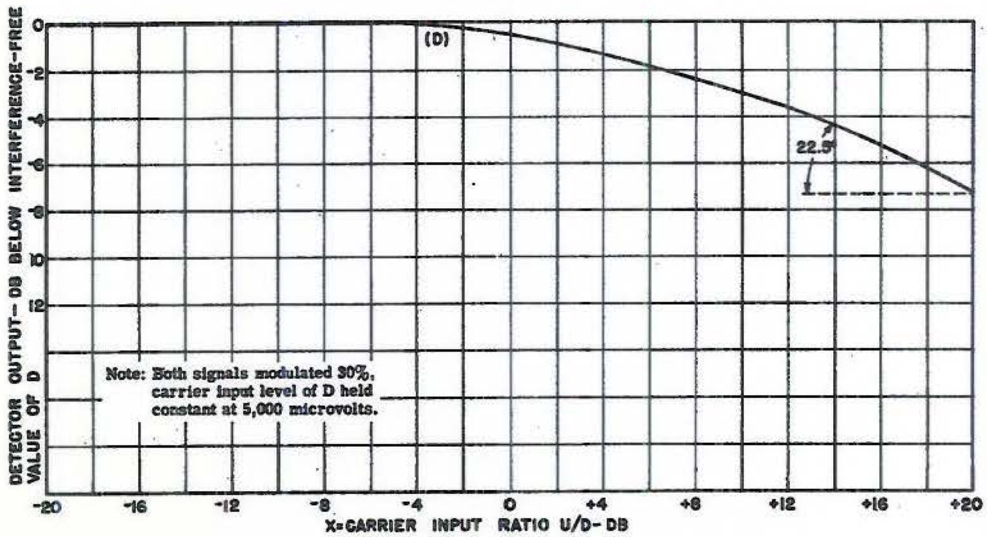

Fig. 3 - Measured capture effect in a-m detector at low input levels (rectification intermediate between linear-law and square-law)

It remains to determine whether the capture effect due to linear-law detection is the same in an f-m receiver as in an a-m receiver. The usual f-m detector uses two balanced half-wave rectifiers whose outputs are connected in voltage or current opposition, whereas a single-ended half-wave rectifier is generally used for a-m detection. The frequency variations of the f-m carrier are converted to amplitude variations in some form of discriminator, the output of which is fed to an amplitude-detection system usually composed of the above mentioned balanced diodes. Amplitude detectors inherently ignore frequency variations, thus leaving for consideration only the amplitude variations present in the output of the discriminator.

Assuming a discriminator composed of two linear and symmetrically opposed slope filters, each feeding one of the two opposed rectifiers, then as the input signal varies in phase or frequency about the mid-frequency of the discriminator, output-voltage variations are produced and passed on to the detectors. For the condition in which the input frequency is at the exact center of the discriminator characteristic, the potentials applied to the two diodes are of equal magnitude, and there is no resultant output from the detector. As the input frequency changes and deviates from the center of the discriminator characteristic, the voltage applied to one diode detector becomes larger and that applied to the other diode smaller relative to the condition at center. The result, over one complete cycle of the input-frequency variation, is a differential output voltage which appears across the detector-output load. With linear slope filters, this voltage can be made to vary almost linearly over a considerable range of frequencies. The fact that the differential detector output is not perfectly linear can be explained by examining the condition in which the instantaneous phase or frequency of the input carrier is at a maximum.

At the peak deviation (maximum frequency excursion) of the input signal on the discriminator characteristic, one diode rectifier is receiving a high potential while the other diode is receiving a considerably lower potential. The diode receiving the higher potential is generally operating in a linear fashion, but the diode receiving the low potential may be operating on the square or an intermediate law region of its characteristic. This is usually true if the input potential to the latter diode is below its internal thermionic-bias potential. Thus the differential output across the detector load in the region of the frequency peaks of input signal may be not quite linear. Of course, the peaks represent a small fraction of the total time of one complete cycle, and therefore the differential output across the detector load can be very close to linear. With two f-m signals present, the capture or depression of the desired signal by the undesired carrier should be essentially no different than that experienced with a single-ended a-m detector insofar as the rectifier portion of the f-m detector is concerned (1 db per db of increase in the ratio U/D in the region where $U/D>1$, when the rms signal-input level is well into the region which produces linear-law detector operation).

Linear Discriminator Analysis (Vector Addition of Input Signals in Absence of Limiting)

The effect of a linear discriminator on capture in an f-m system with no limiting circuits prior to detection will now be considered. Assume that the two input carriers U and D are of identical frequency and are introduced at the center or mid-frequency point of the discriminator characteristic. These input carriers can be represented vectorially as shown in Figure 4 (a), where the vector D is shown stationary and in phase with vector U. Now if the desired carrier, D, is frequency-modulated, it will rotate or wag in first one direction and then the other about the terminus of the undesired carrier, U, as shown in Figures 4 (b) and 4 (c). This rotation of D about U results in amplitude as well as phase-angle variation of the resultant R of the two carriers. Both of these variations affect the response in the output of the discriminator but will be considered separately, the phase-angle variation being treated first.

Consider the discriminator again to be composed of a balanced pair of opposed slope filters. Then, if the unmodulated-carrier frequency (Figure 4(a)) coincides with the center frequency of the discriminator-output characteristic, the condition represented by Figure 4(b) will result in a higher voltage output from one slope filter relative to the other, and that represented by Figure 4(c) will produce the higher voltage output from the other slope filter. If the carrier vector D is "stopped" at an instant of time at which θ is 90°, as shown in Figure 4(d), then by varying the ratio x ($x = U/D$) by changing the length of vector U, the variation in discriminator output produced by variation of the resulting value of phase angle ϕ can be observed. This variation is plotted in Figure 5 based on the simplifying assumption, to facilitate the analysis, that the resultant R maintains a constant amplitude.

Figure 5 shows that the depression of resulting output below its maximum value is 6 db at signal equality ($U/D = 0$ db) with a slope of about 45° in the region where $U/D > 2$. Thus the desired-signal output from the discriminator, resulting from phase-angle variations only, is reduced 1 db per db of increase in the ratio U/D above $U/D = 2$. Stopping the vector D at any other instant of time in its rotation about U would result in a similar curve; the reference or maximum value of ϕ would merely be changed to another angle. Also, stopping the vector D at an instant of time when the resultant is producing the higher voltage from the other slope filter, as shown in Figure 4(e), gives the same curve.

Actually an ideal f-m detector ignores amplitude variations and is responsive only to the frequency variations of the resultant of the two input carriers whose frequency excursions would be represented by the time derivative of the phase-angle variations. M. S. Corrington[11] has developed an expression for the instantaneous frequency of the resultant based on the assumption of two carriers of nearly the same frequency, which are added together to produce a heterodyne envelope resulting from the beating action of the two carriers. This produces, as previously mentioned, amplitude variations as well as variations in phase of the resultant

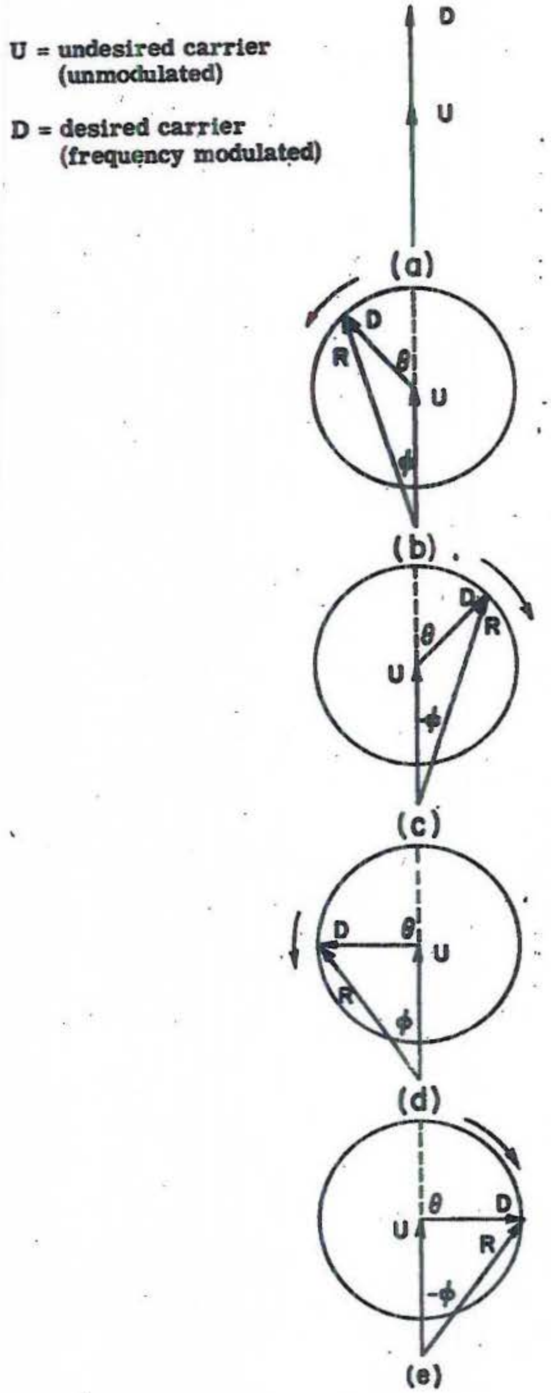

Fig. 4 - Vector addition of two carriers at input to linear discriminator

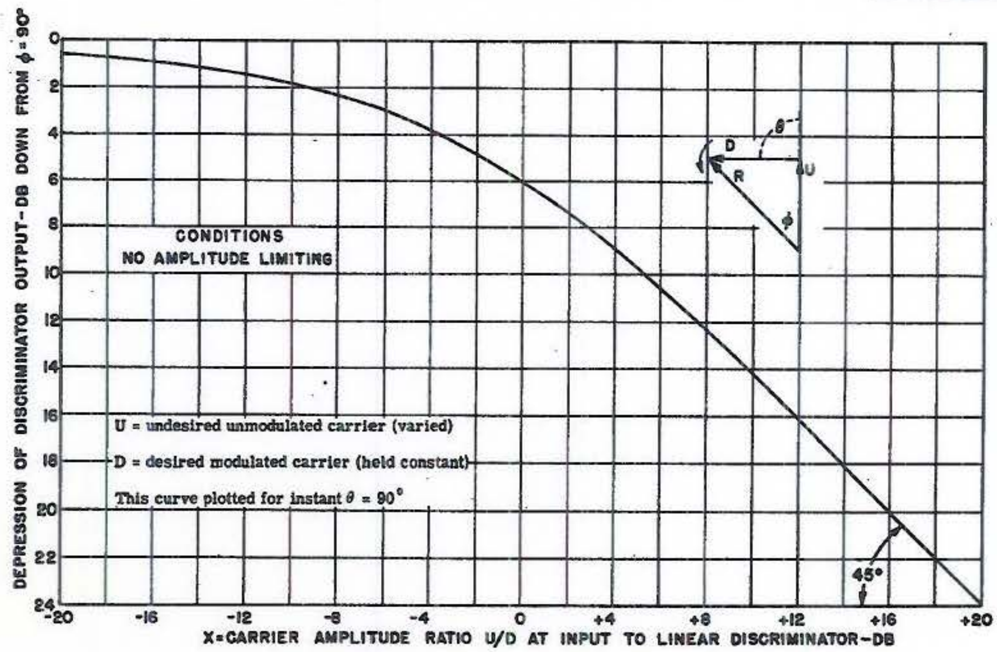

Fig. 5 - Depression of output due only to variation of ϕ at input to linear discriminator. (Derived from vector addition of input carriers U and D based on assumption of constant amplitude for resultant R to facilitate analysis)

the latter representing, in effect, frequency modulation. This analysis will be found in Appendix C. It is only necessary to mention here that, if we assume $\alpha = 0$ and $\cos 2\pi \mu t = 1$ in equation (6C) of this Appendix, then substitution of values for x in this maxima equation leads essentially to the curve of Figure 5. This assumes, however, that the peaks of the envelope are filtered. The minima equation, (7C), of Appendix C becomes indeterminate in the region where $x = U/D = 1$.

The effect on discriminator output of the amplitude variations present in the composite input wave will now be considered. The condition for which the angle θ is 90°, as shown in Figure 4(d), will again be treated. If the U and D vectors are equal in length and in the phase relationship shown in Figure 4(d), the resultant R is 1.414 times or 3 db greater than the amplitude of vector D alone. This amplitude increase, in effect, opposes the 6 db depression due to the phase-angle variation only shown in Figure 5, resulting in an over-all discriminator-output depression of 3 db at input-signal equality. When the undesired signal-input level is one-tenth that of the desired, or U/D = - 20 db, the resultant amplitude is approximately equal to that of the desired signal alone, and the output depression is about as shown in Figure 5, i.e., depression of desired-signal output at U/D = - 20 db is about -0.6 db. When the undesired signal-input level is ten times greater than the desired, or U/D = + 20 db, the resultant is approximately ten times (20 db) greater than the desired signal alone, and the resultant output from the discriminator is increased by about 20 db over that shown in Figure 5. The resulting total over-all depression in the output of a linear discriminator due to the vector addition of two input signals U and D is then as shown in Figure 6. This curve indicates that, in the absence of amplitude-limiting in an f-m receiving system, the maximum over-all depression of a desired signal by an undesired one prior

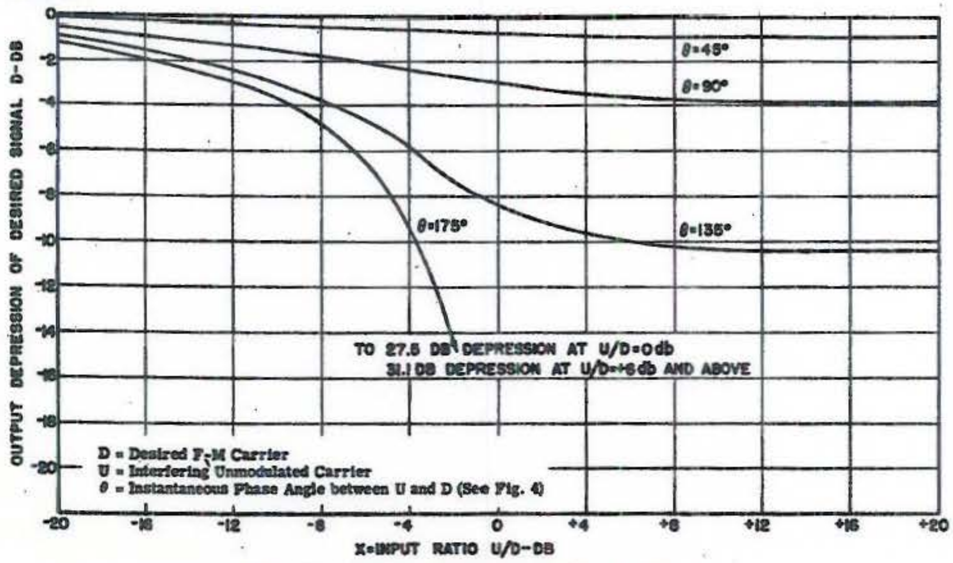

Fig. 6 - Total depression of resultant in output of linear discriminator with no amplitude limiting (derived from vector addition of amplitude and phase variations in input signals)

to rectification is restricted approximately to the value obtained at input-signal equality. The over-all average depression of the desired signal for all ratios of $U/D > 1$ is then about 3 to 4 db.

The above analysis was based on a maximum value for the angle θ equal to 90°. If the desired-signal vector, D, should swing through an angle greater than 90° relative to the undesired vector, U, the over-all depression in the output of a linear discriminator in the absence of amplitude-limiting would be somewhat greater than that shown for the 90° case. This is evident from an examination of Figure 6, where the depressions for $\theta = 135°$ and 175° are also shown. Let us assume that the D vector swings through an angle θ of many thousands of degrees relative to the U vector before reversing direction. The resultant total peak depression in the discriminator output would then be a mean of the curves of Figure 6 for all angles of θ between 0 and 180°, the summation being taken over one complete cycle. This would result in a total threshold depression somewhat greater than the 3 to 4 db specified above for the 90° case. The degree of depression or capture in the region where $U/D > 1$, however, would still be essentially constant, i.e., the curve would be depressed at $U/D = 0$ db, but would have close to a 0° slope for all input ratios of $x > +6$ db. It should be noted that in the region of $X = 0$ db, there is a burst of energy resembling a noise "spike" due to an abrupt reversal of phase at $\theta = 180°$.

Cumulative Capture Effect in F-M System in Absence of Amplitude-Limiting

In the absence of amplitude-limiting, the over-all depression or capture effect in the detector output can be derived from the combined effect of the two input signals on discriminator output added to the previously described detector-rectifier effects. If the rectifiers have a square-law characteristic, the over-all capture curve will be as indicated by Figure 6. If the rectifiers are linear-law, however, the over-all capture would be as in Figure 7, which shows the condition for $\theta = 90°$. The curve of Figure 7 has a slope just slightly greater than 45°. This slight increase in slope is caused by the over-all depression in discriminator

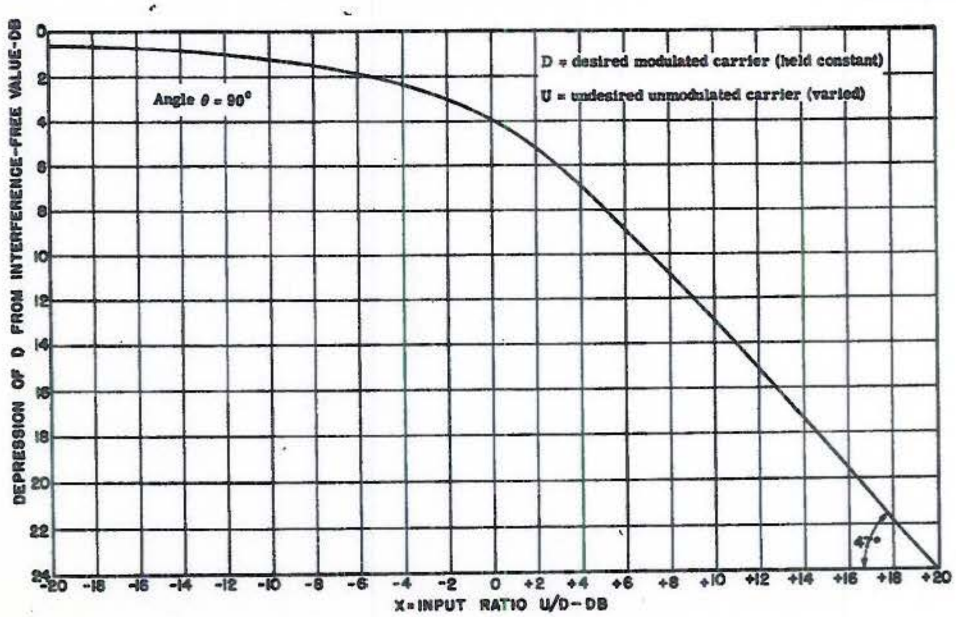

Fig. 7 - Over-all depression of a desired signal in the output of an f-m detector employing linear discriminator and linear-law rectifiers - no amplitude limiting

output before rectification, as previously described and shown in Figure 6. Thus the depression or capture effect in an f-m detector system with linear-law rectifiers in the absence of amplitude limiting is essentially the same as that previously obtained for the a-m detector alone. If square-law detectors are employed, the f-m capture slope is less than 45°, approaching 0° in value, but is depressed by a substantially constant amount in the region above U/D = 1, as compared to the 0° slope and no-depression characteristic obtained with an a-m square-law detector. The results of the above f-m detector analysis without amplitude-limiting have been experimentally verified in the companion report.[4] The curves shown therein appear as Figure 8 of this report. These curves show an average capture slope for the "D" (desired) signal of between 45 and 50° for a "strong" desired signal below the limiting level (linear-law rectification) and a lesser slope (20° to 36°) for a weaker signal providing rectification intermediate between linear-law and square-law.

Amplitude-Limiting

The effects of amplitude-limiting on capture in an f-m system have been previously discussed in the technical literature.[12] The published analyses, however, appear to deal only with the depression of the fundamental-frequency output component of the weaker input signal. It is well known from the law of "conservation of energy" that energy is never actually lost but may be considered as expended in the sense that it has assumed a different form. In the case of amplitude-limiting, some of the input energy is, in effect, redistributed in amplitude and frequency (or phase) by a change of waveform in the output, while the rest of it is dissipated in circuit elements other than the output load. The usual vector representation[13] of the effects of amplitude-limiting upon capture are inadequate, for the simple vector diagram does not show all the redistributed energy appearing in the limiter output. To show this energy distribution, the vector diagram would theoretically have to consist, in many cases, of an infinite but diminishing series of elements having the proper amplitude and phase relationships. Such a diagram, if constructed, would present a confusing over-all physical picture and would be extremely difficult to analyze properly.

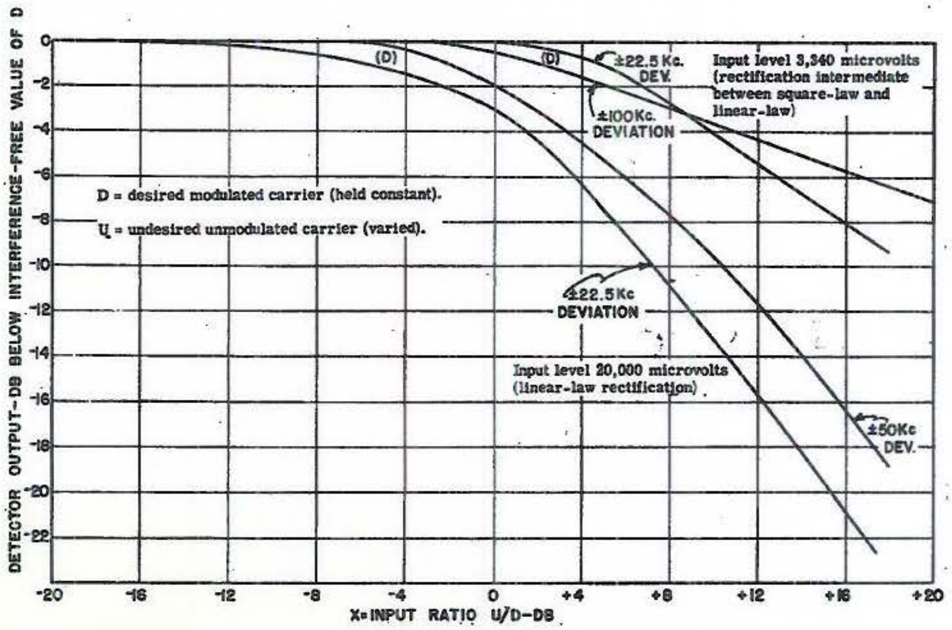

Fig. 8 - Measured capture effect in f-m detector in absence of amplitude limiting

Amplitude limiters can therefore be expected inherently to redistribute some of the input energy of two or more simultaneous input signals in the form of "sideband" energy (complex spectra) in their output circuits. These output spectra can be shown theoretically by a Fourier series, but the analysis to be used in this report is based on the actual measured energy distribution appearing in the output of an effective practical limiter, restricted to the components falling within the average discriminator's useful band.

In Figures 9, 10, and 11 are shown the measured spectra within such a band in the output of an effective one-stage limiter with two-signal input—Figure 9 for equality of input signals, Figure 10 for an input-signal ratio x of 10 (where x = U/D), and Figure 11 for an input-signal ratio x of 0.1. The manner in which these spectrum measurements were made is described in detail in the companion report.[4] Components lower than about 60-db below the amplitude of the maximum component are not shown.

Assume that signal D is the desired frequency-modulated signal, and U the interfering unmodulated carrier, with the further assumption that D and U are of exactly the same frequency and phase when D is unmodulated. Then as D wags about the terminus of U (as previously described in the discussion of Figure 4), the spectrum expands and collapses in frequency about U at the modulation rate of D. Figures 9, 10, and 11 will be taken as representing the situation at the maximum deviation of D below U frequency. The output-frequency separations between all the components shown are equal [(U-D) = (2U-D) - U = (3U - 2D) - (2U - D) = D - (2D - U), etc.], the maximum value of the difference frequency being derived from the maximum phase-angle displacement ϕ (for a given value of the ratio x) of the resultant of the D and U signals.

It is evident from an examination of the input and output spectra of Figure 10 that the fundamental output component of the desired signal D is depressed in amplitude when D is the weaker at the input. At input-level equality (x = 0 db), both the desired and undesired fundamental signal-output components are depressed equally. A plot of the D-signal

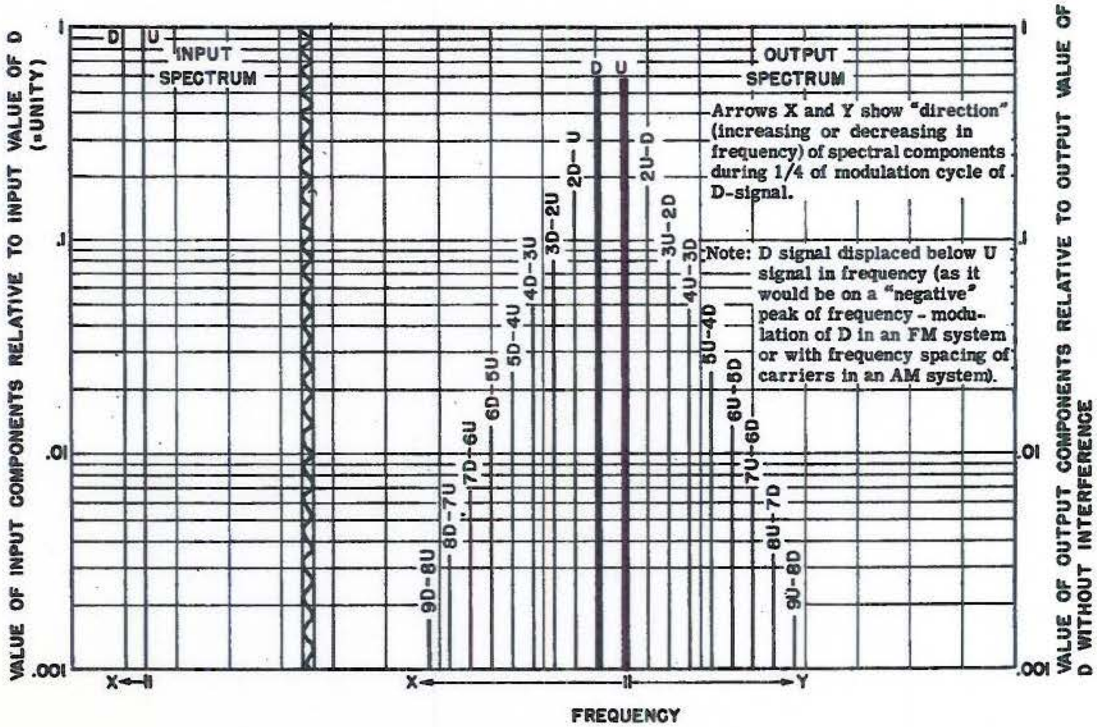

Fig. 9 - Output spectrum produced by effective limiter with two-signal input x = U/D = 0 db

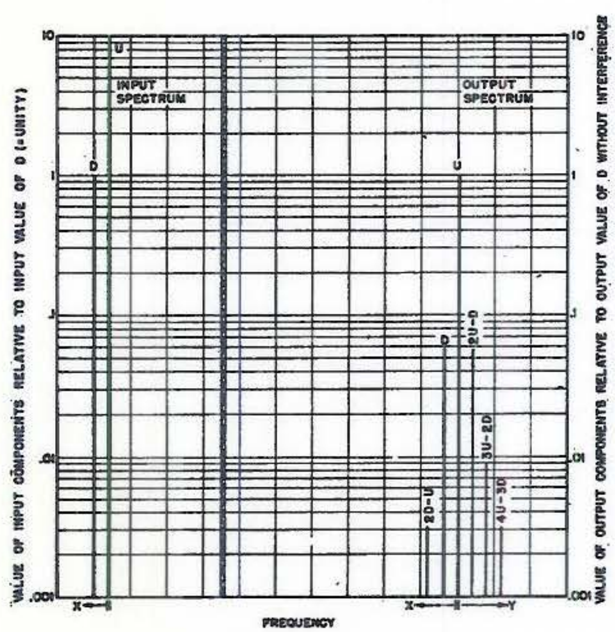

Fig. 10 - Output spectrum produced by effective limiter with two-signal input x = U/D = + 20 db

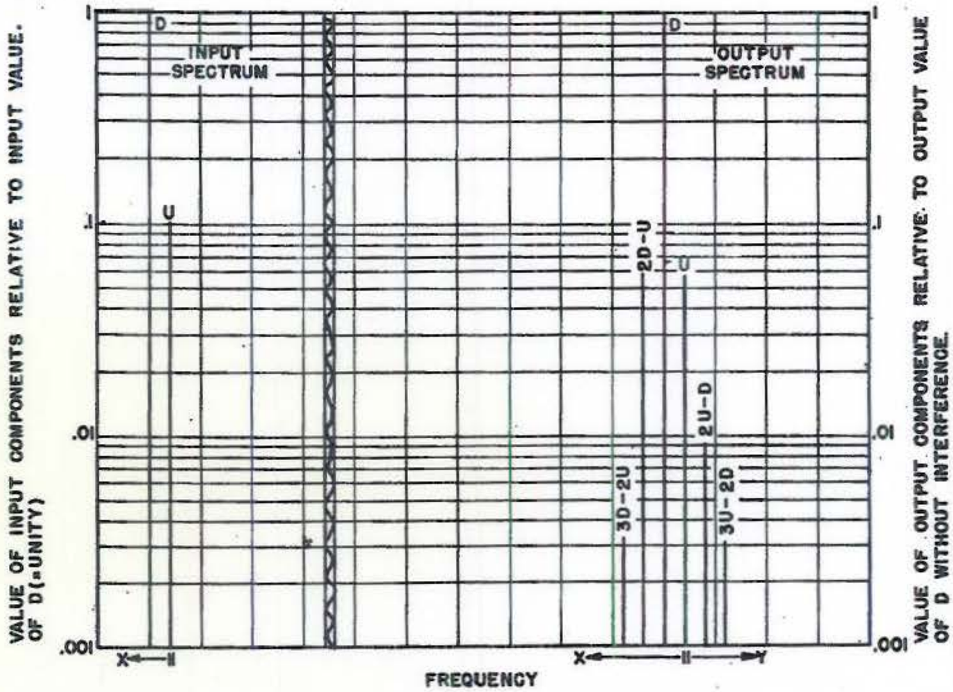

Fig. 11 - Output spectrum produced by effective limiter with two-signal input $x = U/D = -20$ db

fundamental output component depression is shown in the curve of Figure 12 and again in the experimental curve of Figure 13. The depression at $x = 0$ db is roughly 5 db relative to the D signal without interference, and the slope of the curve in the region where $x > 0$ db is 45°. Figure 13 also shows a plot of the next strongest components appearing in the limiter output, i.e., 2D - U and 2U - D. These have a much greater depression at $x = 0$ db and a slope of about 60°. Similar experimental curves will be found in the companion report.[4] The 45° capture slope of the fundamental component of D in the limiter output, as shown in Figures 12 and 13, is in agreement with the results already published in the technical literature[12] and also with those previously discussed for the case of a linear-law detector. It must be remembered, however, that the discriminator is receiving a spectrum of energy, not just the fundamental components of input signals D and U appearing in the limiter output.

The following analysis shows the resultant of the limiter-output components in the output of an f-m detector. This detector will be assumed, as before, to consist of a pair of linear slope filters, followed by a pair of square-law rectifiers, each filter connected to its own rectifier, with the rectifier-output circuits connected in opposition. The resultant discriminator characteristic is assumed to be a straight line. The output spectrum shown in Figure 10 will be considered first with the unmodulated U-signal component centered on the discriminator cross-over or center-frequency. As previously mentioned, the D component in Figure 10 is shown at maximum or peak deviation from its unmodulated frequency, the latter being of the same frequency and phase as U. The U-signal component produces identical rectified-current values in each slope filter and rectifier circuit, whereas the D, 2U - D, 2D - U, etc. components produce a net rectified-current value which is higher in one slope filter and rectifier circuit than in the other. This is due to the unbalance of

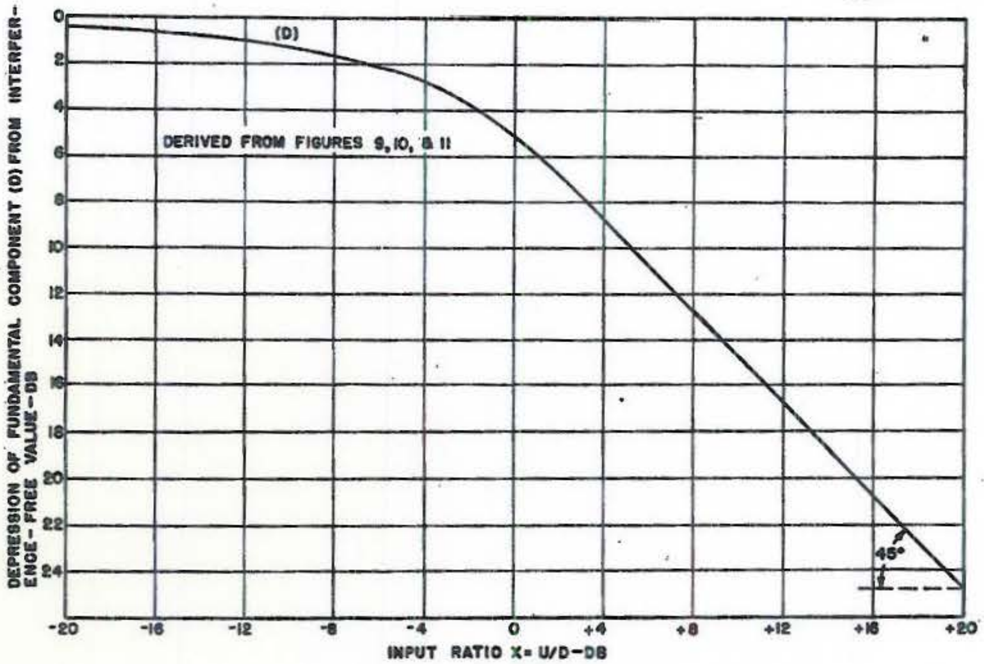

Fig. 12 - Depression of fundamental component (D) in output of effective limiter

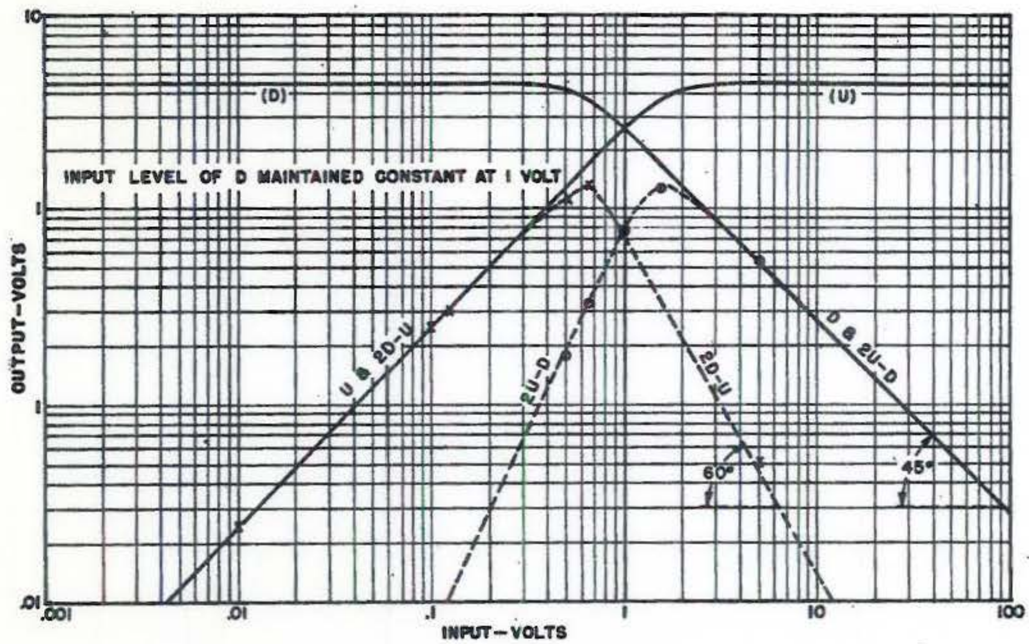

Fig. 13 - Experimental curves showing depression of D, U, 2U-D, and 2D-U signal components in output of effective limiter

spectral energy appearing on the two sides of U signal, as shown in Figure 10. The frequency spacing and "direction" of deviation of each of these components relative to the U signal (Figure 10) must be considered, as well as their relative amplitudes in computing the residual output.

The output from the slope filter and rectifier circuits due to components D and 2U - D cancel, since they are of the same amplitude, are "spaced" in frequency symmetrically [U - D = (2U - D) - U] about U, and are moving in opposite "directions" in frequency during modulation due to the build-up and collapse of the spectrum during the modulation cycle of the D signal. The amplitude of component 2D - U is less than that of 3U - 2D, leaving a net amplitude differential due to 3U - 2D. This differential must be multiplied by the factor 2 to find the resultant output, since both 2D - U and 3U - 2D are two frequency units [2 (U - D)] removed from the center-frequency U and generate twice as much net rectified voltage in the discriminator output as components at one-unit spacing. Component 4U - 3D appears alone on the "high" side of U in the spectrum shown. Actually there is a component 3D - 2U, not shown, also at three frequency units removed but on the "low" side of U. Its amplitude, however, is small and it can be ignored without introducing appreciable error. Component 4U - 3D must therefore be multiplied by the factor 3, since it is three frequency units removed from U. The total effective residual voltage is then equal to the differential of the net voltages derived as described above. This net residual voltage appears in the combined output of the rectifiers. The relative phases and absolute frequencies of the spectral components at the input to the rectifiers is unimportant, since only the variations in rectified current generated by their change in frequency relative to U appear in the output, modified by the variations in instantaneous amplitude corresponding to the "beat" between the D and U signals.

As previously stated, the output spectrum shown in Figure 10 represents the significant energy appearing in the output of the limiter under one condition (ratio $x = +20$ db) of two-signal input. Components 60-db or more below the maximum-component level and harmonics of D and U (i.e., 2D, 2U, etc.) have been ignored. Each spectral component may be thought of as being produced by a separate generator having zero impedance and feeding the discriminator and its rectifiers through the effective plate resistance of the limiter. The principle of superposition then allows separate treatment of the rectifier output due to each generator, as shown above for the square-law rectifier case. For this case, as previously shown with two signals, there is no depression of one signal by another due to the rectifiers themselves, and the various components can be combined directly with no correction for rectifier capture effect.

The resulting computed over-all capture of signal D, as derived from the spectra of Figures 9, 10, and 11 for square-law rectification, is shown in Figure 14. The curve shows 5-db depression of desired-signal output at $x = 0$ db and a slope of roughly 59° in the region where U is stronger than D. On the basis of a more exact Fourier-series analysis, the above capture slope would approach $\mathrm{Tan}^{-1} 2$ or 63.5°. The spectra (Figures 9, 10, and 11) used in the construction of the 59° curve were obtained by measurement, and the low-amplitude components existing considerably removed in frequency from the center-frequency U were subject to appreciable measurement error and were therefore ignored. The harmonics of D and U (2D, 2U, 3D, etc.) were also ignored as being entirely outside the discriminator pass-band.

The over-all capture in the output of an f-m detector employing linear-law rectifiers in place of square-law rectifiers (assuming one stage of effective amplitude-limiting as before) can be determined as follows. Since the capture slope for an f-m detector employing square-law rectifiers is in the region of 63.5°, the substitution of linear rectifiers which, as previously discussed, themselves have a 45° capture slope results in a total over-all slope of approximately $\mathrm{Tan}^{-1} 3$ or about 71.6°. This is plotted in Figure 15, where the

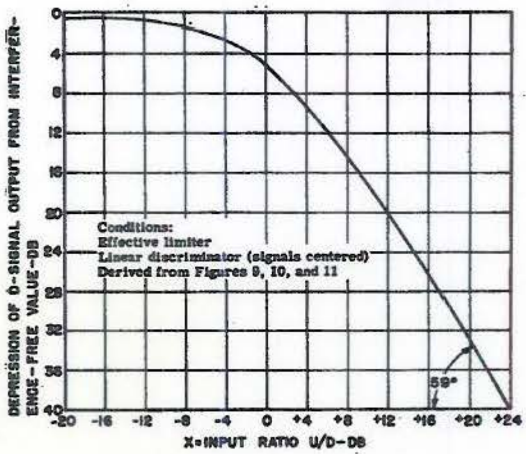

Fig. 14 - Depression of desired-signal output resulting from summation of all significant spectrum components of (D) signal in output of linear discriminator - square-law rectifiers assumed

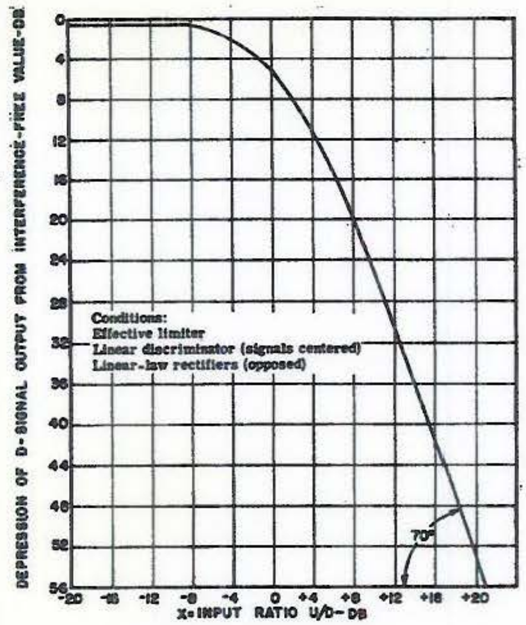

Fig. 15 - Depression of (D) signal in output of linear-law f-m detector

depression at input-signal equality is again 5 db and the slope in the region where U/D> 1 is roughly 70°. This capture slope should approach 71.6° as a limit on the basis of more exact spectral measurements.

Cascaded Limiters

The effect on capture of cascading limiters can now be considered. The second limiter will receive at its input the type of output spectrum illustrated by Figures 9, 10, and 11, instead of just the two original signals appearing at the input to the first limiter. The case in which $x = U/D = 10$ or + 20 db, as shown in Figure 10, will be examined with regard first to the output spectrum from the second limiter as produced by the D and U components, then to the output spectrum produced by the 2U - D and U components, and finally to that produced by the 2D - U and 3U - 2D components. The addition of these spectra results in a new over-all output spectrum from the second limiter. The 4U - 3D component also produces a family of spectral lines in the second limiter output, but these will be ignored as negligible in calculating the depression of the output from the original signal D.

Figure 16(a) shows the second limiter output spectrum produced by the D and U output components (spectrum of Figure 10). Figure 16(b) shows the same thing for the 2U - D and U components of Figure 10. Figure 16(c) shows the resulting output spectrum from the second limiter derived by addition of the amplitudes of the components having the same frequency in Figures 16(a) and 16(b). Similar spectra are shown in Figures 17(a) and 17(b) for input components 2D - U and 3U - 2D, with Figure 17(c) again showing the resulting output spectrum derived by addition. Figure 18 shows the over-all spectrum resulting from all the components as it appears at the output of the second limiter (Figure 16(c) + Figure 17(c)). This spectrum, when impressed on a discriminator centered at the U signal, followed by linear-law rectifiers, gives an output attenuation of 72 db for $x = 10$, or a capture slope of 73.5°. This represents an increase in slope of only 3.5° over that for one limiter stage (Figure 15). In other words, increasing the number of limiters in cascade does not greatly increase the capture effect.

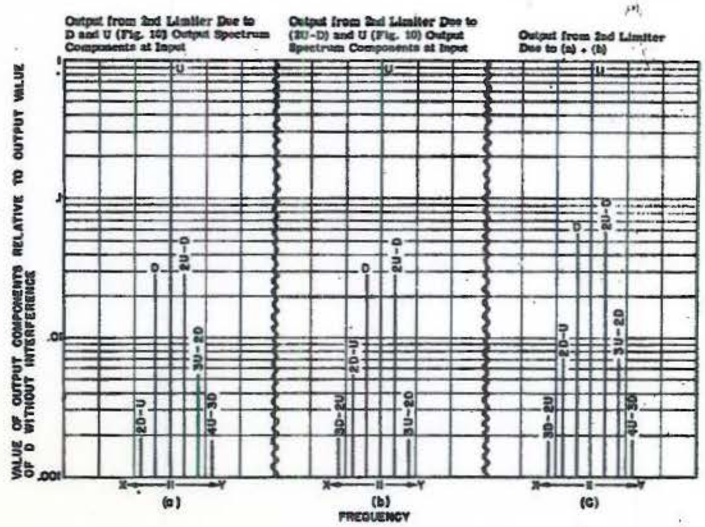

Fig. 16 - Spectra output from 2nd limiter due to D and U, (2U-D) and U (Figure 10) output spectrum components at input

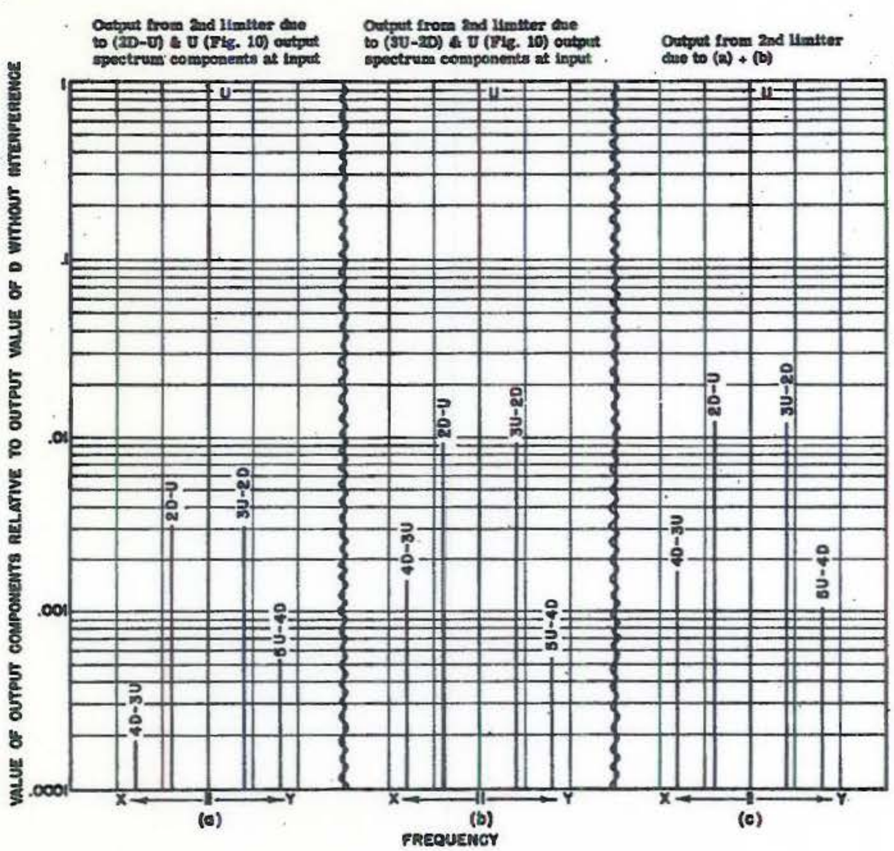

Fig. 17 - Spectra output from 2nd limiter due to (2D-U) and U, (3U-2D) and U (Figure 10) output spectrum components at input

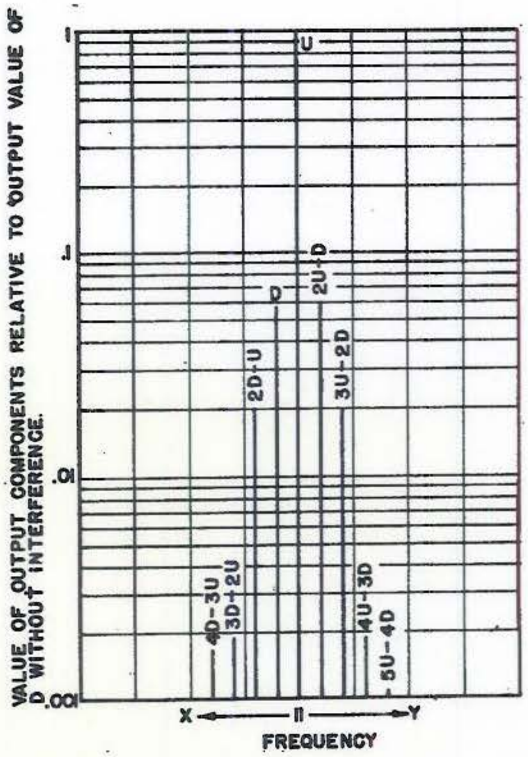

Fig. 18 - Output from 2nd limiter due to addition of spectra of Figures 16(c) and 17(c)

It is evident that all limiting prior to detection must be eliminated to insure minimum capture in an f-m receiver. With limiting, minimum capture will be obtained when the greatest practicable bandwidth is provided at the discriminator stage itself. Experimental verification of the effect of additional limiting will be found in the companion report,[4] as well as in following pages of this report. If a single limiter stage provides poor limiting, however, then additional cascaded limiting will be useful as a means for correcting the deficiencies of the single limiter. But it is generally possible to approach a practical ideal in f-m limiting with a single full-wave shunt-connected limiter employing crystal diodes which have inherently low "contact" potential. This limiter should be located just prior to the discriminator for maximum effect.

Automatic Volume Control (A-M and F-M)

As is well known, the purpose of automatic volume control in an a-m receiver is to hold the average audio output constant when the input signal is "fading," or otherwise varying in level, and to prevent excessive average audio-output level change when the receiver is tuned from a weak signal to a strong one, or vice versa. The d-c component of the rectified carrier is generally used to provide the controlling voltage for the AVC system. This rectifier may be the signal detector itself or a separate unit intended for AVC purposes only. The AVC rectifier usually controls only the gain of the amplifiers preceding the final detector by means of a d-c feedback loop, which regulates the control-grid or other electrode d-c potentials of the individual amplifier stages. This gain-regulating process is well known and needs no further explanation here. It remains, however, to determine how the AVC system affects the relative depression of one signal by another in the audio output under conditions of two-signal input to the receiver.

The curves of Figure 19 show typical AVC characteristics. Curve (A) represents an ideal condition, for the output is absolutely constant for all increases in signal-input level beyond the AVC threshold value. Curves (B) and (C) represent less effective AVC action, with the audio output increasing for increased signal-input level, although at a much slower rate than for the case of no-AVC as represented by curve (D). Curve (E) represents voltage-delayed AVC action, i.e., the AVC control voltage is delayed in its application to the d-c feedback network until a certain predetermined input-signal level is reached (higher AVC threshold). Incidentally, curve (B) may be made to approximate ideal curve (A) by the application of some AVC voltage to the amplifiers following the final detector.

If the AVC characteristic is ideal, as exemplified by curve (A) of Figure 19, the input to the final detector is restricted in level, therein resembling the limiting previously discussed for amplitude-limiters in an f-m system, but with a relatively long time-constant and no intentional distortion of the amplitude-modulation envelope. The output depression

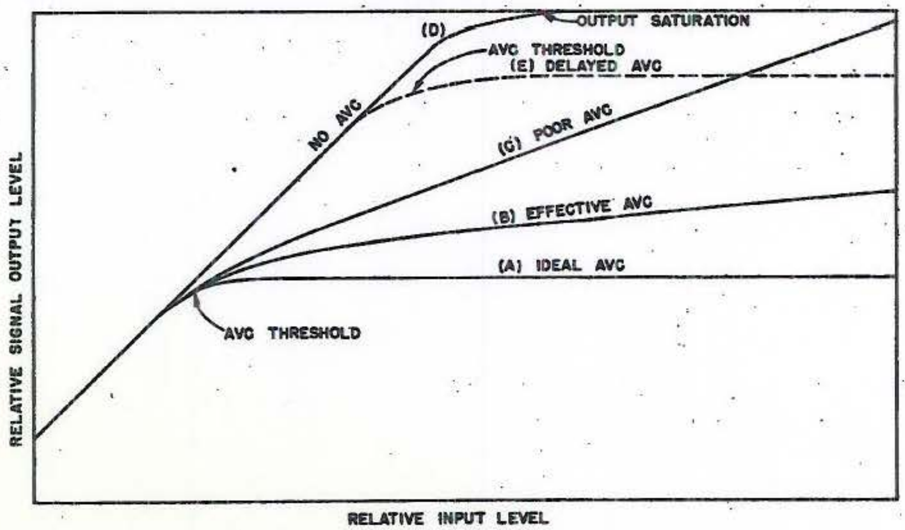

Fig. 19 - Typical AVC characteristics

of the weaker of two input signals due to AVC action alone will be about as shown in Figure 7, where the capture slope is 45°. With AVC characteristics as represented by curves (B) and (C) of Figure 19, the capture slope due to AVC action becomes less than 45° until, under the conditions of no-AVC shown by curve (D), the capture slope due to AVC action alone is 0°. With delayed AVC, represented by curve (E), the capture slope due to AVC alone is 0° for the weaker input-signal levels up to the threshold of AVC action and 45° for strong input-signal levels above that threshold. The over-all capture in an a-m system above the AVC threshold resulting from the combination of ideal AVC action and linear-law detection will be as shown in Figure 20. This curve has a 63.5° capture slope and represents the maximum capture normally obtainable with low-output distortion in an a-m receiving system.

In an f-m system, the effect of AVC on capture is minor when effective amplitude-limiters are employed. It should be noted, however, that voltage-delayed AVC should be used, so that the limiting threshold is well exceeded before AVC action begins. This is particularly important in the case of poor limiting, where nondelayed AVC may prevent limiter input amplitudes from reaching effective levels. In f-m receivers which have excellent limiter design, properly designed AVC can be very useful by serving to maintain limiter and discriminator input at more nearly constant levels, thereby insuring that the angle of conduction of both limiter and rectifier tubes remains more nearly fixed. This can be an important

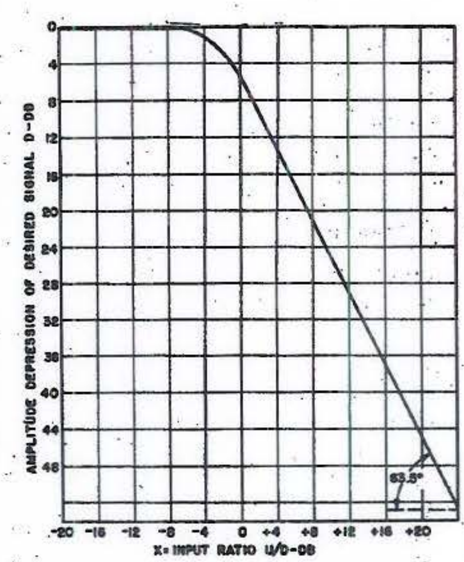

Fig. 20 - Maximum capture in a-m system with ideal AVC characteristic and linear-law rectification

element in minimizing detuning effects due to tube input impedance changes and in maintaining the amplitude-rejection and downward-am characteristics of the receiver at desirable values. If the AVC characteristic is ideal and the limiting is effective, the spectral input to the discriminator should be essentially no different from that shown in Figures 9 through 18, provided that the input levels of the signals at the limiters are above the limiter threshold. If the AVC characteristic is poor, limiter-input levels will vary more. Capture effects may remain essentially the same but detuning effects due to tube input-impedance changes will be greater.

AFC Circuits and Noise-Peak Limiters

There are several other circuit arrangements used in a-m receiving systems which may be termed capture or anti-capture devices, such as automatic-frequency-control (AFC) networks and noise-peak limiters. AFC circuits are normally used in a-m receivers in which maintenance-of-tuning difficulties exist due to frequency drifts in the system. Such receivers generally utilize a frequency-detector which develops a d-c voltage proportional to the frequency difference between the signal frequency as actually applied to the frequency discriminator and the center-frequency of the discriminator characteristic. The resultant d-c voltage usually controls a "reactance" tube, which in turn controls the heterodyne-oscillator frequency in the case of superheterodyne receivers. The actual circuits used in such AFC systems are well known and will not be shown here. In the presence of an undesired stronger signal off the desired-signal frequency, the AFC can cause the oscillator to be "pulled" so that the undesired signal is at resonance, while the weaker desired signal may be substantially detuned. Thus the signal of the greater amplitude may capture the receiver in frequency. This can be a very serious effect, depending on the frequency separation and the amplitude difference between the desired and undesired signals. The AFC system can aggravate an existing capture effect due to amplitude differences by further increasing the difference in amplitude between desired and undesired signals through the medium of detuning.

Noise-peak limiters are anti-capture devices in that they can prevent noise pulses or interfering signals of the impulse type from capturing a receiver through masking of the desired signal in the receiver output. In this respect it would perhaps be better to think of noise limiters as "amplitude-selective anti-capture devices," i.e., amplitude-selective in that they suppress only modulation peaks above a predetermined threshold value, anti-capture in that they prevent impulse noise from masking or suppressing output signals of the voice-modulation type. AFC can also be made "anti-capture" by inverting its action to discriminate against the stronger signal.

Effect of Nonlinear and Nonsymmetrical Discriminator Characteristics

The effects of nonlinear and nonsymmetrical discriminator characteristics on the over-all capture slope will now be considered. The output spectrum of Figure 10 will be assumed present at the input to the discriminator. In Figure 21(a) is shown a seriously nonlinear discriminator characteristic. If component U of Figure 10 is at the center of this characteristic, the amplitude differential between components 2D - U and 3U - 2D must be multiplied by something less than the factor 2. Although these components are still two frequency units removed from the center, U, the output is no longer directly proportional to the input-frequency differential between the individual components. Likewise, component 4U - 3D must be corrected in amplitude by a factor determined by the curvature of the discriminator characteristic and considerably less than 3. The over-all net desired-signal output from the discriminator, therefore, will be somewhat less than that previously shown for the linear discriminator case. Thus the resultant depression or capture of the desired signal, D, in the discriminator output is greater than the 33 db shown in Figure 14. With a curvature of the discriminator characteristic the reverse of that shown in Figure 21(a), the over-all net output would be somewhat more than that previously shown for the linear discriminator. Thus the resultant depression of the desired signal, D, in the discriminator output would be less than the 33 db shown in Figure 14.

If the spectrum of Figure 10 is off center on a linear discriminator characteristic (U component no longer at center), the residual amplitude of all the output components due to modulated signal D at the input will still remain the same and the over-all capture slope will be substantially unchanged. Except for serious nonlinearity, this can also be substantially true for the nonlinear but symmetrical discriminator.

If the discriminator characteristic is nonsymmetrical, as shown in Figure 21(b), then, with the input spectrum of Figure 10 centered at U frequency, the components on the high-frequency side of U will produce a maximum voltage from one slope filter and the components on the low-frequency side of U will do likewise with the other slope filter, as previously explained. The amplitude differential between the 2D - U and 3U - 2D components, however, can no longer be multiplied by a common amplitude correction factor as before. Instead, each component amplitude on one side of U must be multiplied by one factor before subtraction and each component on the other side of U by another factor, due to the nonsymmetry of the discriminator. The resulting capture will be dependent on the spectrum composition and its location (centered or noncentered) on the discriminator characteristic. In Figure 22 is shown the computed effect on capture of detuning the spectrum of Figure 10 on the nonsymmetrical discriminator characteristic illustrated in Figure 21(c), assuming U frequency centered for zero detuning. It is evident that the minimum degree of capture occurs with U signal centered (zero detuning) and that the degree of capture increases rapidly with relatively small detuning until all the output-spectrum components of Figure 10 fall on one slope of Figure 21(c). Thereafter the degree of capture

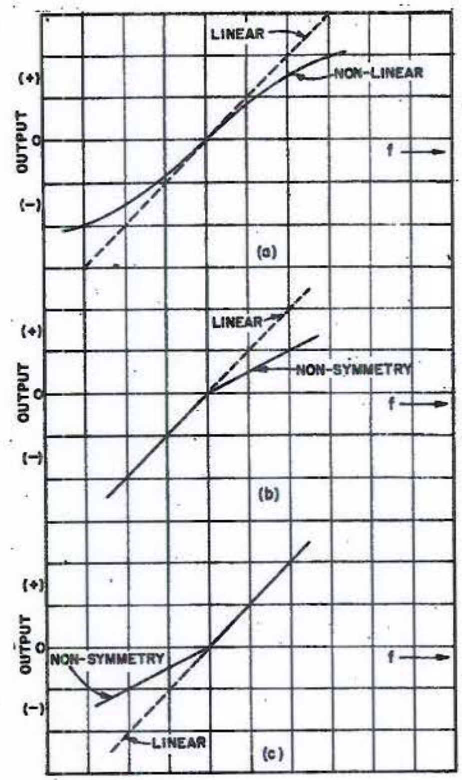

Fig. 21 - Nonlinearities and nonsymmetries of discriminators

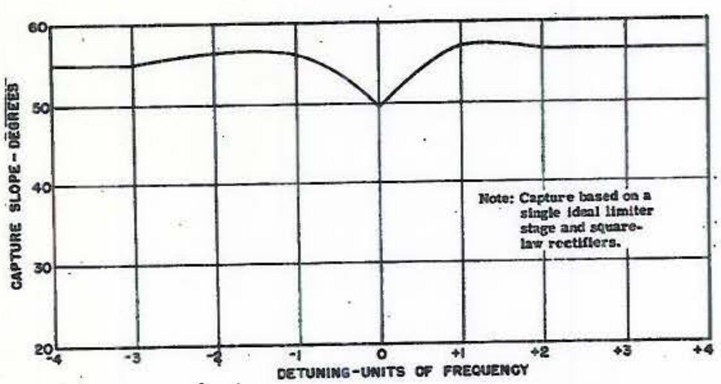

Fig. 22 - Computed effect on capture of detuning the spectrum of Figure 10 on a nonsymmetrical discriminator characteristic (Figure 21(c)) - U-frequency centered for zero detuning

remains constant for all further increments of detuning. Thus the greatest reduction in capture obtainable with a seriously nonsymmetrical discriminator should occur with the input spectrum centered at or near the center of the discriminator characteristic. With relatively large detuning, the degree of capture should be essentially no different from that experienced with a linear discriminator characteristic.

Combination of Effects Influencing Capture

The curves of Figure 23 show the resultant limits of capture for the specified conditions of receiver circuitry, as derived from the considerations in the preceding sections of this report. The curves, for the most part, are self-explanatory and summarize the capture slopes to be obtained from purely theoretical considerations of receiver circuitry. These slopes will be tabulated in greater detail in the final summary, along with experimental verification as given in the following sections of this report.

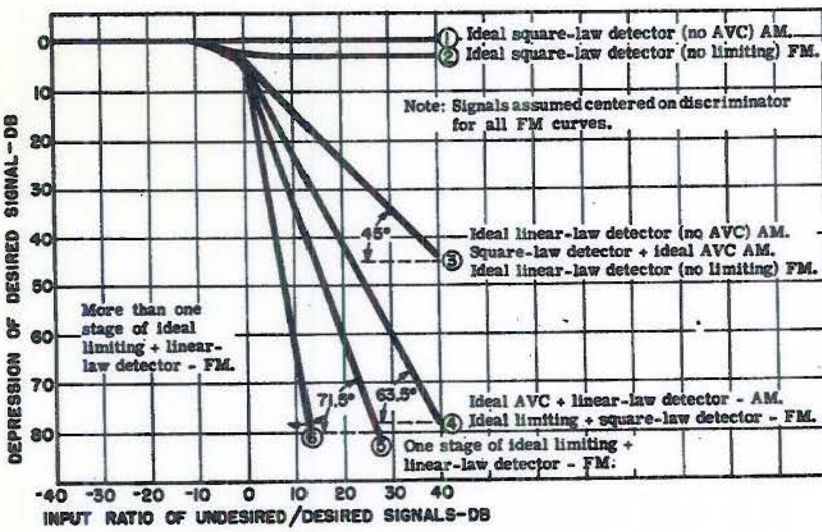

Fig. 23 - Theoretical capture curves for f-m and a-m receivers

EXPERIMENTAL ANALYSIS

In substantiation of the preceding theoretical analysis,? considerable experimental data has been compiled and analyzed. For purposes of investigating capture due to the f-m detector alone, a typical Foster-Seeley phase-discriminator was used, as shown in Figure 24. The 6AC7 driver tube was intended for purposes of preamplification only and not as a limiter. Since limiting was absent with input levels below the saturation threshold of this stage, the capture effects observed can be attributed to detector action alone for such levels of input.

For purposes of determining the f-m capture due to limiting, a Navy Model X-RDZ-2 receiver was employed. This receiver uses a ratio-type detector, as shown in the circuit diagram of Figure 25. In order to provide a more effective limiter in this circuit, a pair of 1N35 germanium crystals were used as a full-wave shunt limiter. This limiter circuit is also shown in Figure 25.

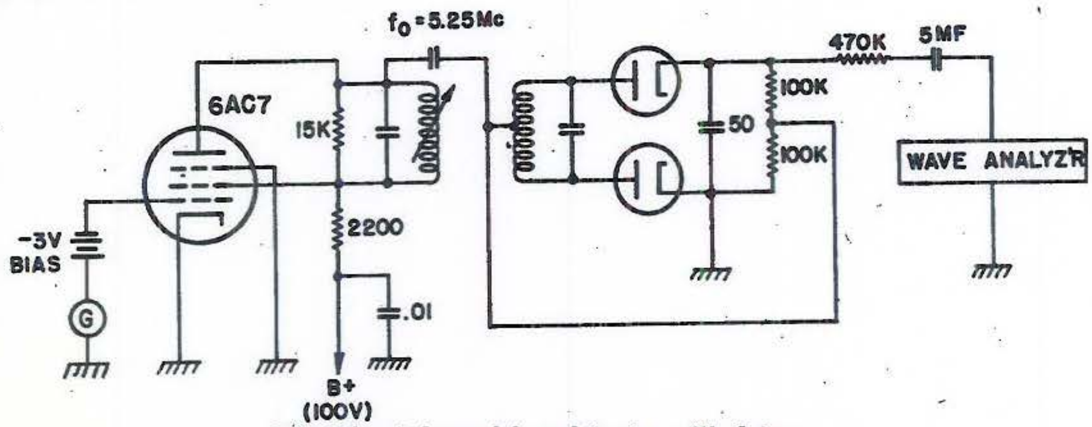

Fig. 24 - Balanced f-m detector with driver

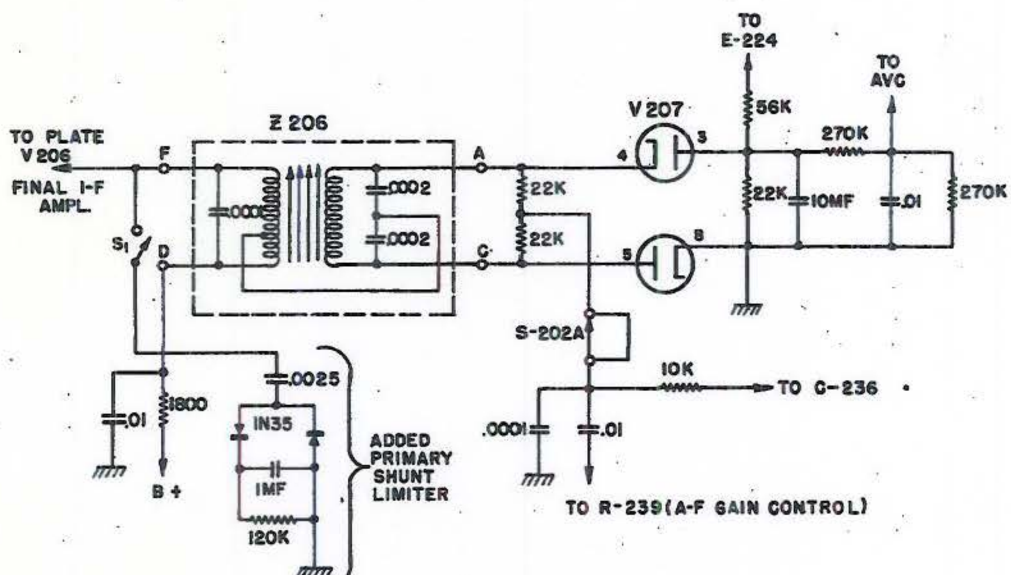

Fig. 25 - Ratio detector with primary shunt limiter

In order to approach the no-limiting condition, the circuit of Figure 25 was altered to that of Figure 26. This modification attempted to abrogate the half-wave shunt-limiting inherent in the ratio detector, but some limiting action still remained, particularly for frequencies above 1000 cps. For the purpose of analysis, however, this circuit has been labelled the "no-limiting" case.

A-m measurements were made on the same receiver as used for FM by replacing the discriminator transformer of Figure 25 with the usual Model RDZ final i-f transformer and making one of the two detector diodes inoperative. This modified circuit is shown in Figure 27.

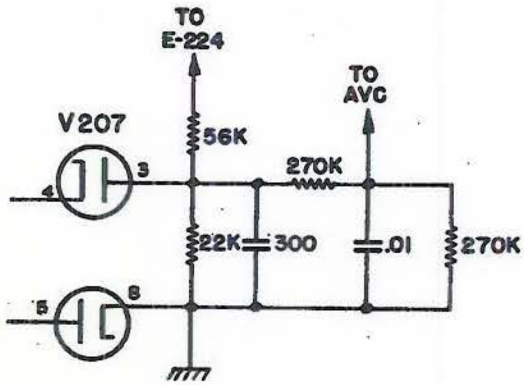

Fig. 26 - Detector modification for "no-limiting" case

In order to determine the effects of the degree of limiting on the capture phenomenon, it was decided to investigate first that "two"-signal operation condition in which only the desired signal was injected from an external source into the receiver, the undesired or interfering signal being the fluctuation noise contributed by the circuits preceding the final detector. Capture would then be indicated by the relative slopes of the output signal-to-noise ratio curves for the various conditions of limiting.

The output measurements were made with a Hewlett-Packard Wave-Analyzer and a Ballantine Electronic Voltmeter (100 kc bandwidth) connected in parallel. This arrangement was employed to enable more exact determination of output S/N ratio at the low-input levels. The Ballantine meter read the true signal-to-noise ratio only for output levels above about +10 db output S/N, whereas the Wave-Analyzer could read the true output-signal level down to about -39 db S/N due to its much narrower bandwidth (6 cycles) but was not suitable for output-noise measurements because of that narrow bandwidth. A correction factor, based on the ratio of the two meter readings at low-input levels, has been applied to obtain the S/N curves of this report. This factor was computed in the following manner.

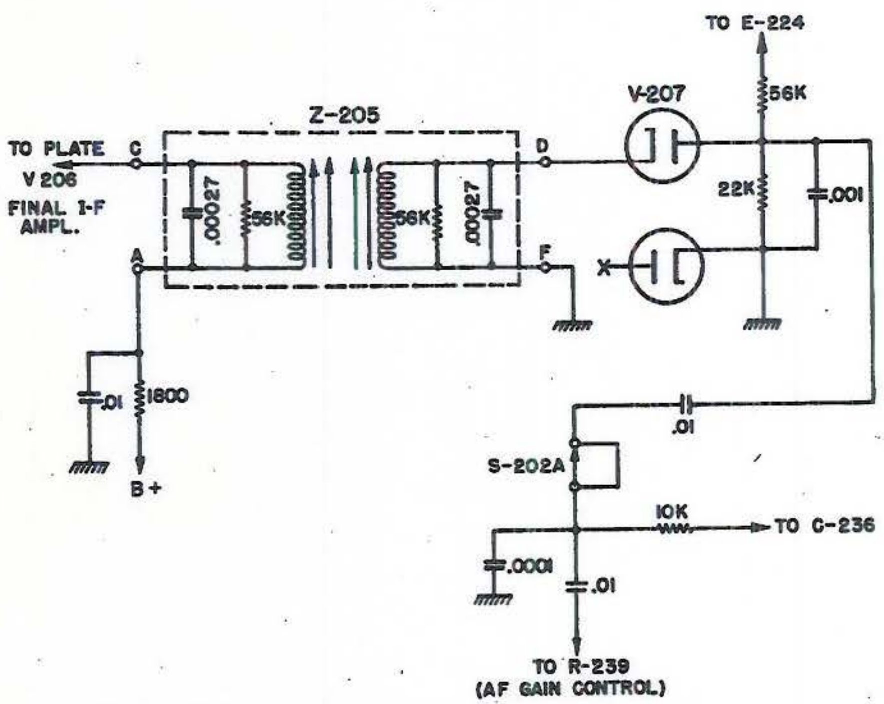

Fig. 27 - X-RDZ-2 detector as modified for a-m measurements

Let E_1 = Ballantine Meter reading (which is rms) = $\sqrt{S^2 + N^2}$ (4)
where S = rms signal output only and N = rms noise output only.

Let E_2 = Wave-Analyzer reading = S (rms value of the signal only down to receiver output S/N value of -39 db). Then

$$N = \sqrt{E_1^2 - S^2} \text{ (from equation (4))} \tag{5}$$

and

$$S/N = \frac{S}{\sqrt{E_1^2 - S^2}} .$$

Dividing top and bottom of the right side of equation (5) by S gives

$$S/N = \frac{1}{\sqrt{(E_1/E_2)^2 - 1}} . \tag{6}$$

For the particular instruments used, the resultant S/N ratio will be accurate to not better than about 0.5 db for receiver output S/N ratios of -40 db or greater. The true S/N ratio can quickly be determined from the instrument readings with the aid of the curve of Figure 28.

Analysis of Output Signal-to-Noise Characteristics

In Figure 29 are shown curves of the output S/N ratios for various conditions of limiting as the input level of the externally injected signal is increased. The input signal was fed to the grid of the first detector stage of the X-RDZ-2 receiver from a Boonton Model 150A f-m signal generator externally modulated by a Hewlett-Packard Model 200B audio oscillator. The audio output was measured on a Model 300 Ballantine Electronic Voltmeter and a Model 300A Hewlett-Packard Wave-Analyzer connected in parallel, as previously discussed. All the f-m output S/N curves were taken with ± 7.5 kc deviation and 1000 cps sine-wave modulation. The 6-db bandwidth of this particular X-RDZ-2 receiver used was approximately 105 kc. The r-f gain control was held constant at maximum gain and the a-f gain control was initially adjusted to give +20-db output S/N ratio at 6-MW output (1.9 volts across the 600-ohm output load). For all of these measurements, the audio and i-f selectivity controls were in the "narrow" position (audio 6-db nominal bandwidth = 350 to 3500 cps; i-f 6-db nominal bandwidth = 125 kc) with the AVC and noise-limiter off. All of the curves have been corrected by use of Figure 28 to provide true S/N ratios below +10-db receiver output S/N ratio.

The primary shunt-limiter introduced an insertion loss of approximately 3 db (as measured below the threshold of limiting). The addition of this limiter circuit across the primary of the discriminator transformer also resulted in a slight detuning of that winding. This was corrected by adjustment of the primary tuning slug.

It is evident from examination of the curves of Figure 29 that the addition of the primary shunt-limiter results in an improved output S/N ratio from the f-m receiver as compared to the ratio detector only. This added limiter, while not a perfect limiter in the strict sense of the term, nevertheless represents a single effective limiter stage which approaches the ideal. It was found that the cascading of additional limiters of this general type in progressive i-f amplifier stages prior to the final i-f amplifier resulted in no measurable improvement in output S/N over that represented by the single added primary limiter curve of Figure 29. It should be remembered that the ratio-detector itself is a half-wave shunt-limiter, which is supplemented by the added full-wave shunt-limiter, and that the

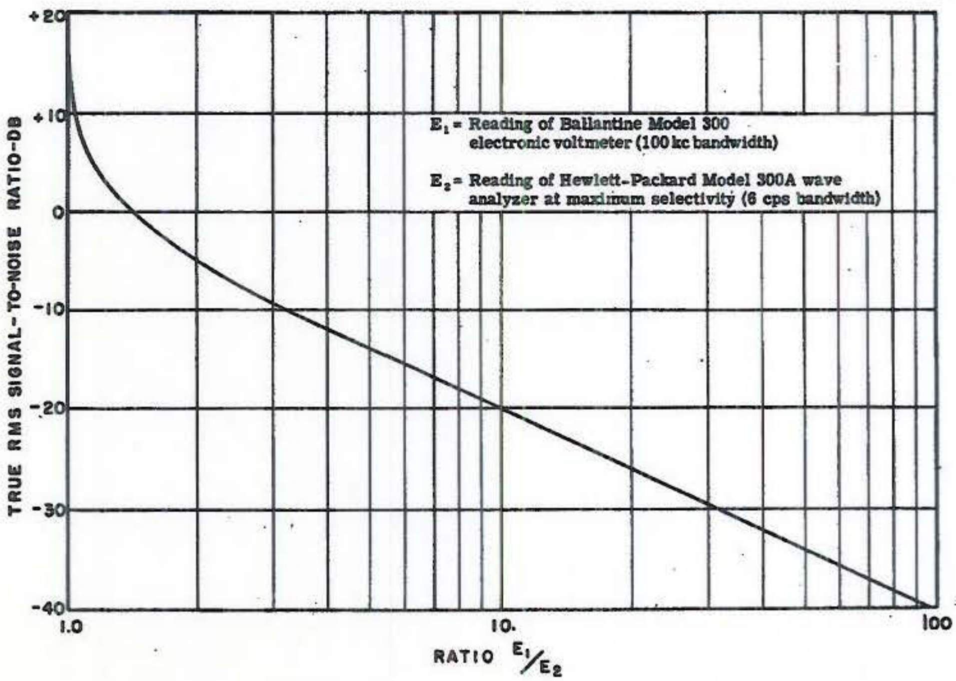

Fig. 28 - True output signal-to-noise (S/N) ratio

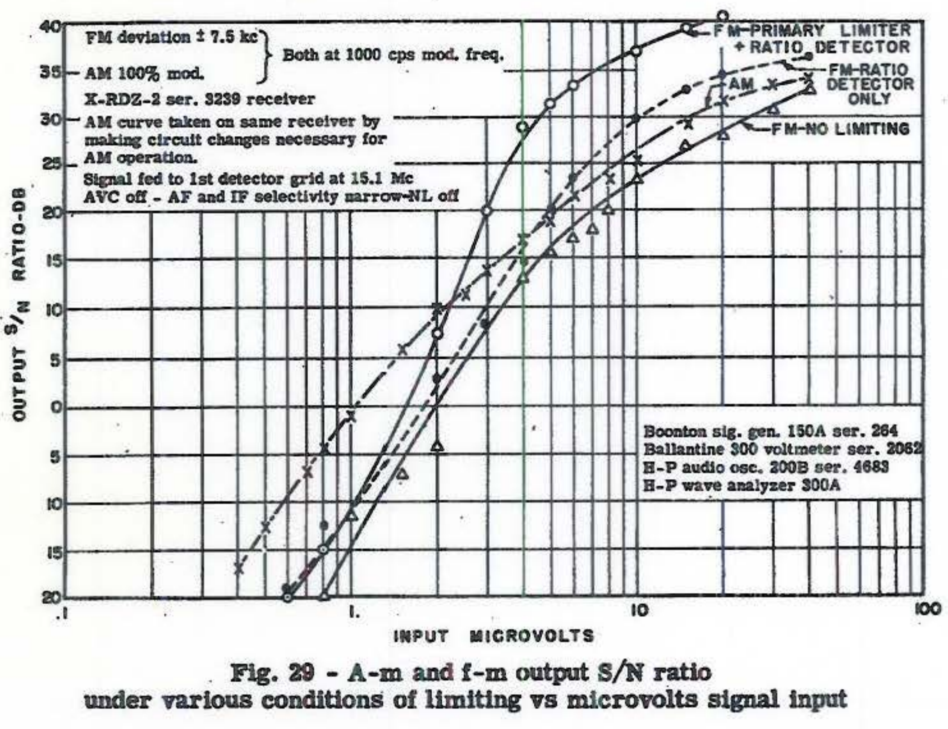

Fig. 29 - A-m and f-m output S/N ratio under various conditions of limiting vs microvolts signal input

i-f amplifier stages preceding the detector would saturate in turn as the input-signal level increased. The main effect of the added primary-side limiter would then be to provide full-wave limiting in the input region below the input value at which i-f amplifier saturation becomes effective (about 50 microvolts). Since the internal thermal voltage of the full-wave crystal limiter used is low (about 0.2 volt or less), this would mean that effective limiting, approaching the theoretical zero-threshold ideal, would be obtained down to very low input levels. The ratio-detector limiting threshold is determined by the thermionic-bias of its diodes, about 2.5 volts as compared to about 0.2 volt for the crystal-diode pair.

The curves of Figure 29 show that between the extremes of limiting, as represented by the "primary-limiter plus ratio-detector" and the "no-limiting" curves, there can be various degrees of improvement in output S/N due to limiting action. One intermediate condition is represented by the "ratio-detector only" curve. The half-wave shunt-limiting inherent in that type of detector represents a degree of limiting which is not completely effective but which nevertheless is much better than no limiting at all.

The improvement in output S/N ratio of FM over AM at the higher input levels is also evident from these curves. The "ratio-detector only" curve crosses the "a-m" curve at an output S/N ratio of about +18 db. Above this point, f-m output S/N ratios are better, while below this point AM is superior. The "primary-limiter" curve crosses the "a-m" curve at an output S/N ratio of about +10 db. Thus the effect of adding a single effective full-wave limiter circuit to the f-m receiver is to extend the f-m S/N ratio improvement range to lower input levels.

The slopes of the "f-m no-limiting" curve and the "a-m" curve of Figure 29 measure roughly 40°. The slope of the "ratio-detector only" curve is about 57°, while that of the "primary-limiter plus ratio-detector" curve is roughly 70°. These slopes will later be compared to the slopes of other experimental capture curves. It should be noted that the curves of Figure 29 are very similar to typical capture curves, with the U/D ratio decreasing to the right instead of to the left and with the U signal held constant.

The S/N curves of Figure 30 were obtained in a manner similar to that used for the curves of Figure 29 except that a higher deviation (30 kc) was employed in the f-m measurements. The average slopes of these curves are nearly the same as those of Figure 29, the main differences appearing in the higher output S/N ratios obtained at the medium- and high-input levels due to higher deviation.

De-Emphasis

In Figure 31 are shown output S/N curves as taken with a de-emphasis filter connected between the plate of the second detector and the grid of the first a-f amplifier for both the a-m and the f-m cases. The time constant of this r-c de-emphasis network was chosen to produce output attenuation starting at 500 cps and reaching 6 db per octave above 2000 cps, as shown in the audio-response curves of Figure 32. The addition of this network to the receiving system results in a higher over-all output S/N response for both AM and FM. This can be seen by comparing the curves of Figure 31 with those of Figure 29 for corresponding conditions of limiting. Both of the f-m curves at 2-microvolts signal input are increased about 1 db in output S/N ratio, while the a-m curve is improved by +3 db. At 10-microvolts signal input, the "ratio-detector plus shunt-limiter" curve is improved by +3 db, while the "ratio-detector only" and the "a-m" curves are improved by about +5 db. Thus de-emphasis (which postulates transmitter pre-emphasis) improves the output S/N response of both systems, with the a-m receiver benefitting to a greater degree than the f-m receiver. There is a slight but negligible increase in the slope of the output S/N curves with the addition of de-emphasis. Thus the capture slope of the curves is essentially the same as that without the de-emphasis network.

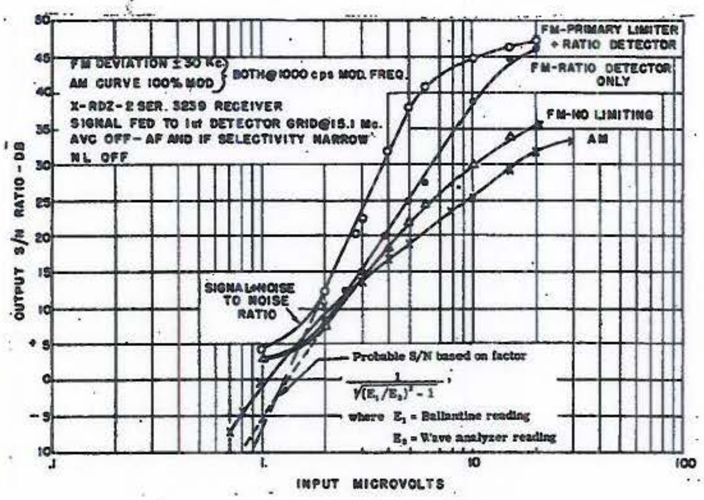

Fig. 30 - A-m and f-m output S/N ratio under various conditions of limiting vs microvolts signal input

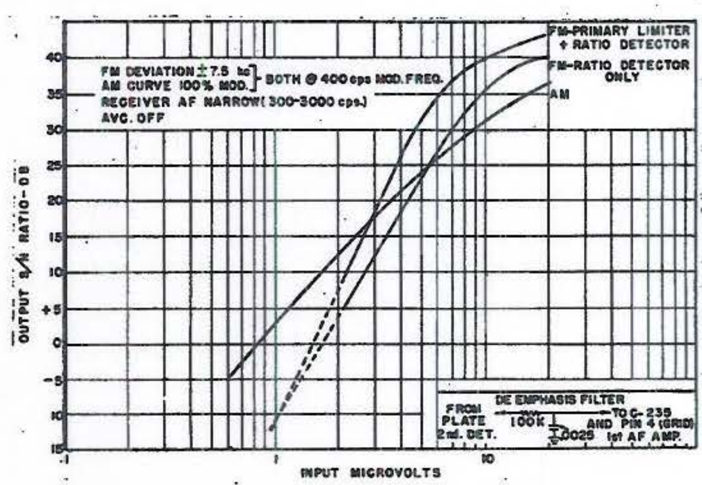

Fig. 31 - Output S/N response with de-emphasis

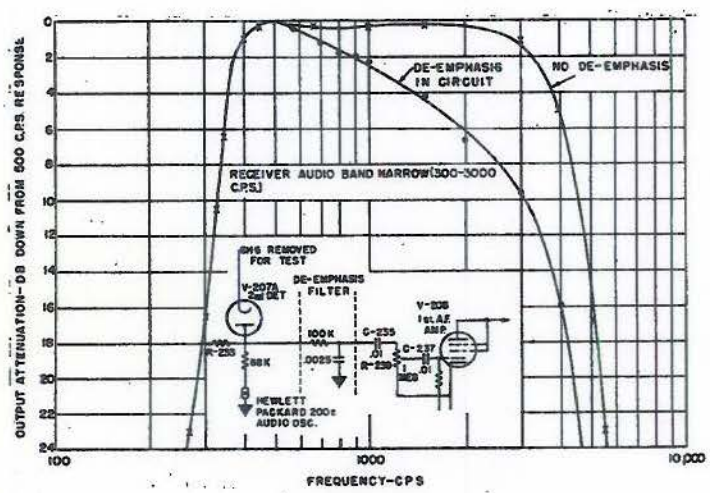

Fig. 32 - Audio response of X-RDZ-2 receiver with and without de-emphasis

Detuning

Figures 33-37 show the effects of carrier detuning on f-m receiver performance. These measurements were made by feeding a 15.1-Mc signal modulated ± 7.5 Mc at 1000 cps to the mixer grid of the receiver from a Boonton Model 150A signal generator. The degree of detuning from the "resonant" or center-frequency input point was determined at the same time by feeding the unmodulated carrier output from the signal generator for each point measured into a General Radio type LR-1 Heterodyne-Frequency-Meter and Crystal-Calibrator. The output S + N/N ratio measurements were made with a Ballantine Electronic Voltmeter (Model 300). It is not essential that the detuning curves be given a detailed analysis in this report. They will be discussed briefly, however, since general inferences as regards capture can be drawn from their examination.

The detuning curves of Figure 33 show that, aside from the increase in output S + N/N ratio obtained at the lower input levels with more effective limiting, the deteriorations of S + N/N ratio due to detuning are more severe at low-input levels with the ratio-detector plus primary-limiter than with the ratio detector only. This can perhaps be seen more clearly from the curves of Figure 34, where the output S + N/N ratios have been plotted on a relative-attenuation basis. It is evident from an examination of Figures 35 and 36, which show the noise output and the signal output separately, that this effect is due primarily to a greater increase in the noise output with detuning in the case of the ratio-detector plus primary-limiter than in the case of the ratio-detector only. Further examination of the curves reveal that, at higher input levels, the noise is substantially constant across the pass-band of the receiver prior to final detection for both cases of limiting, and that the output S + N/N ratio change with detuning at the higher (50-microvolt) level is essentially the same for both cases to the limits of the pass-band. At the higher input level, the decrease in output S + N/N ratio with detuning is due mainly to signal-output attenuation.

Figure 37 shows the effect of detuning on the output signal-to-noise ratio of actual f-m receivers, as exemplified by the Model X-RDZ-2, compared to theoretical detuning curves as computed on the basis of a rectangular selectivity characteristic. It can be seen that the reduction in output S/N ratio for a given degree of detuning from center is greater for the "ratio-detector plus primary-limiter" curve than for the "ratio-detector only" curve. This indicates that a receiver with a near-ideal limiter is susceptible to a greater degree of capture with detuned signals than is one with a less effective limiter as represented by the ratio-detector alone. In the latter case the signal is captured by noise. Similar capture effects will occur at the higher input levels where noise is low but an interfering carrier is present instead.

Capture Curves

Figure 38 shows the discriminator characteristic obtained with the circuit of Figure 24. The data for this curve was obtained by feeding an unmodulated carrier to the grid of the driver stage from a Boonton Model 150A signal generator. The d-c output voltage of the discriminator-rectifiers was measured with an R.C.A. Volt-Ohmist Jr. The discriminator center-frequency was 5250 kc. Using the circuit of Figure 24, capture effects were measured such as shown in Figures 39 and 40. These measurements were made primarily to determine the effect on capture of the f-m detector circuits alone. Since there was no low-level limiter element in this network, any capture effect present should have been due mainly to linear detector action alone, as long as the driver-stage input levels were well below the values at which that stage began to saturate. Signal U was provided from a Boonton Model 150A signal generator modulated externally by a Hewlett-Packard Model 200 audio oscillator at 2000 cps with the carrier-frequency set at 5250 kc. Signal D was

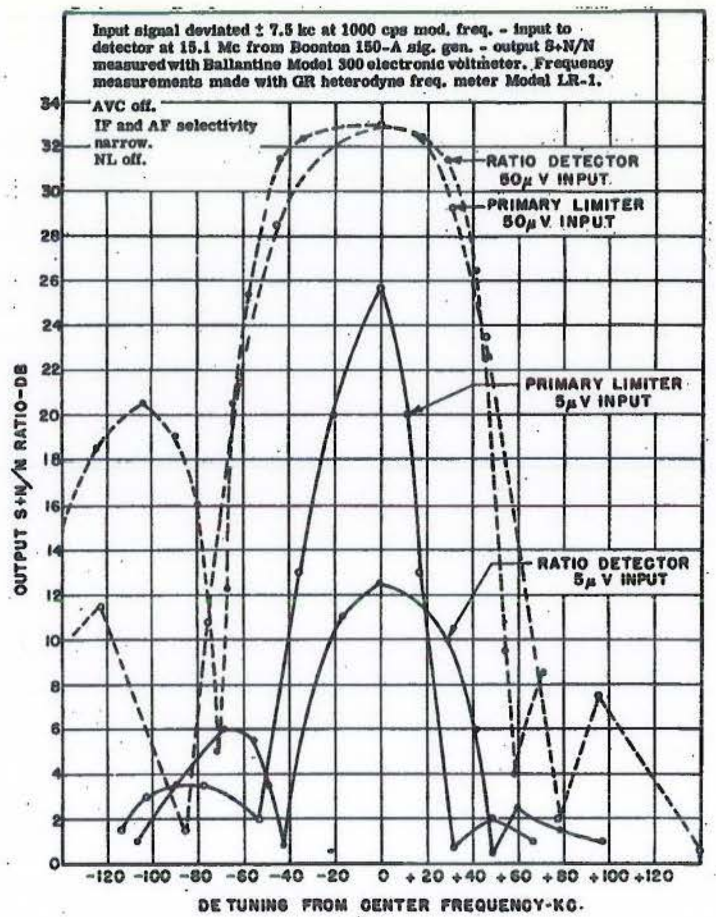

Fig. 33- Effect of detuning the carrier from the center-frequency of an f-m receiver

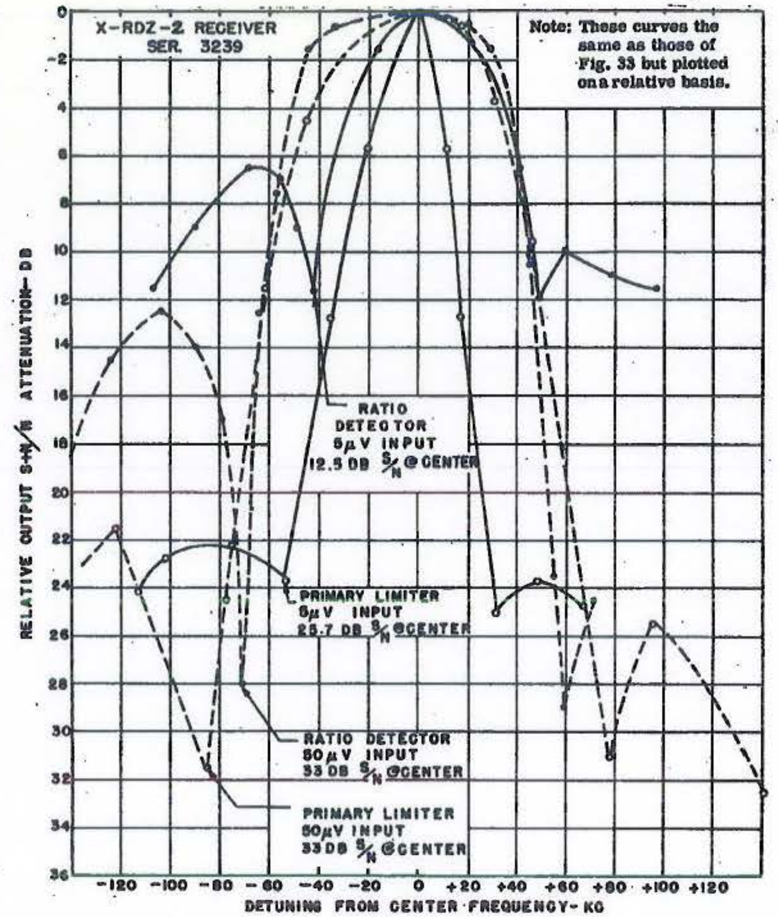

Fig. 34 - Effect of detuning the carrier from the center-frequency-curves plotted on relative attenuation basis

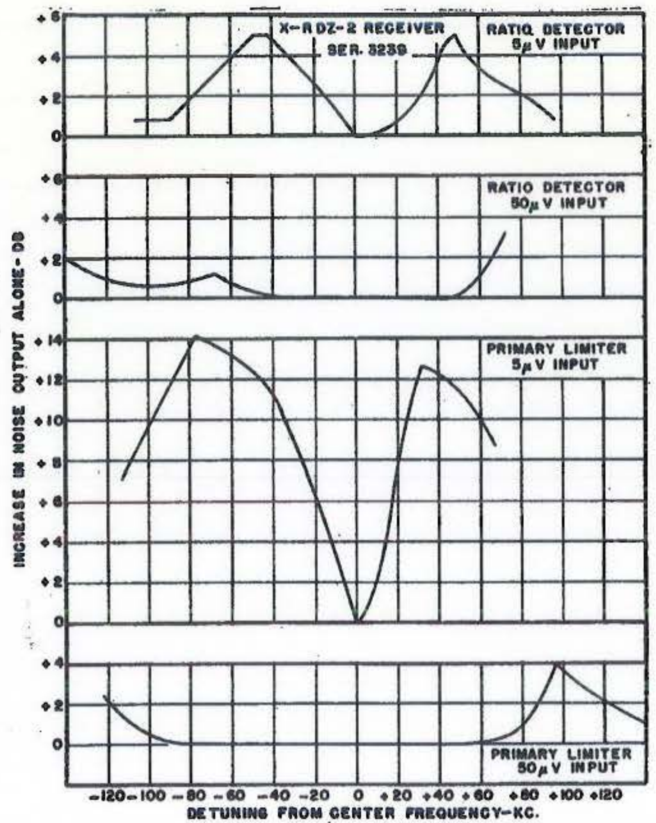

Fig. 35 - Effect of detuning on noise output alone

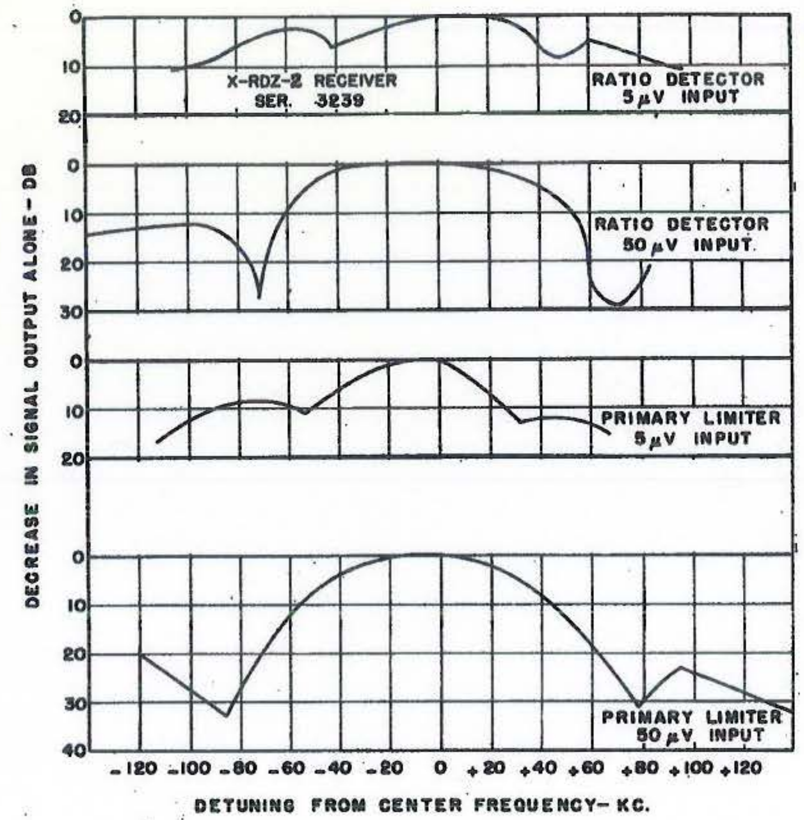

Fig. 36 - Effect of detuning on signal output alone

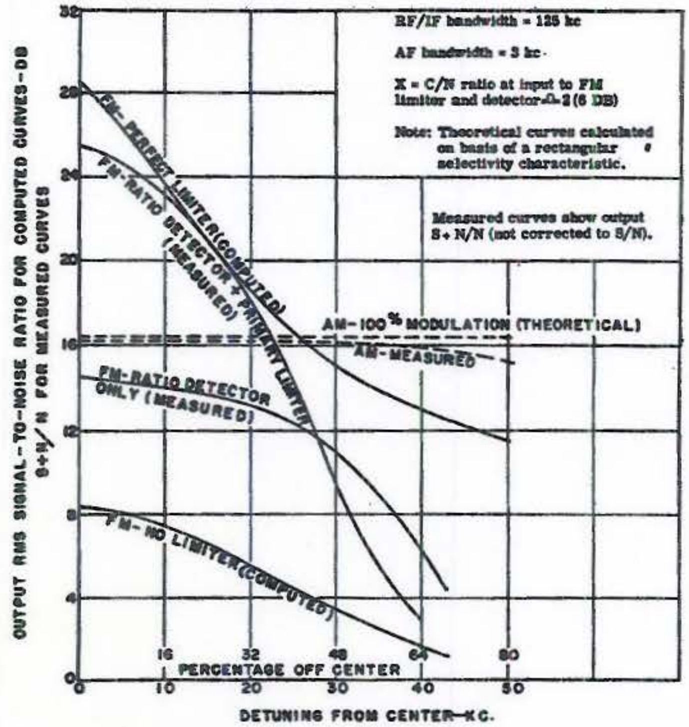

Fig. 37 - Comparison of effects of detuning as measured to theoretical limits

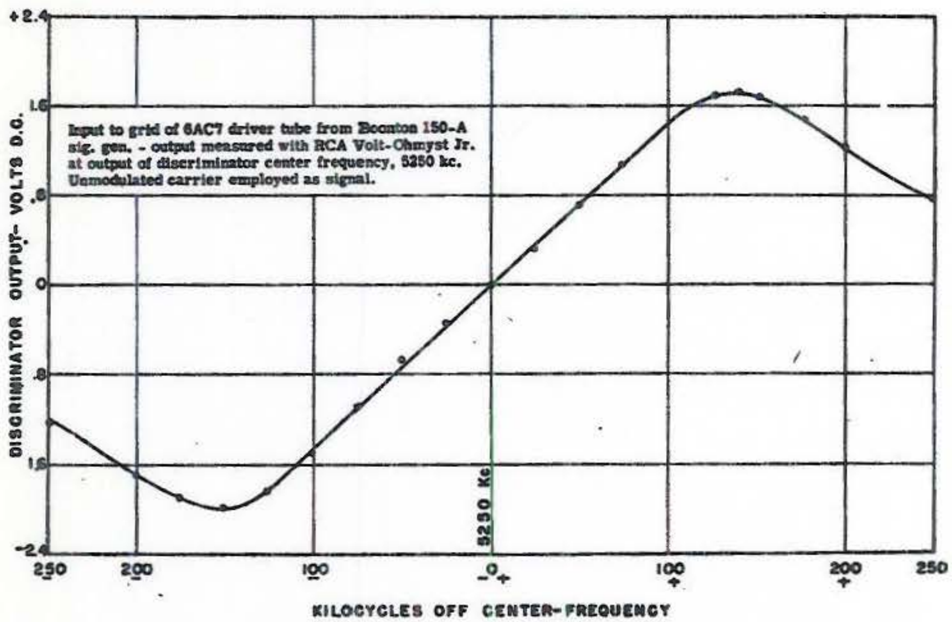

Fig. 38 - F-m discriminator characteristic

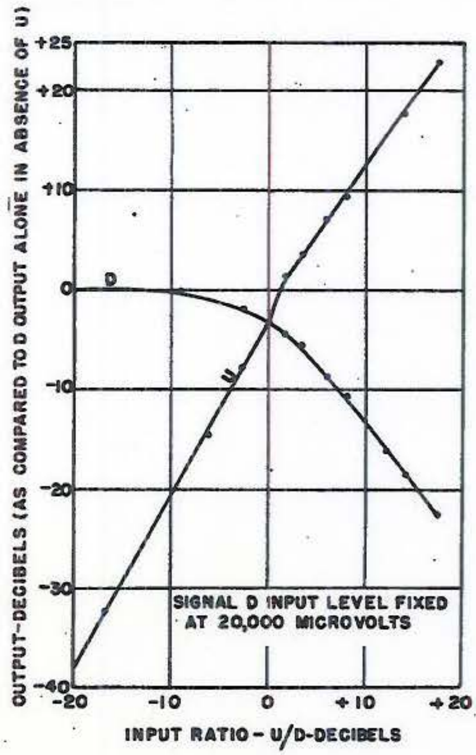

Fig. 39 - Measured capture effect in f-m detector alone - ± 22.5 kc deviation

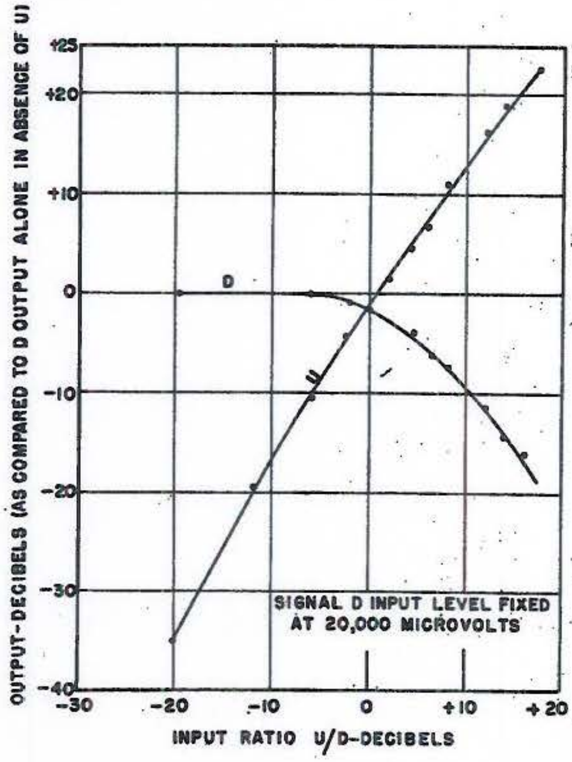

Fig. 40 - Measured capture effect in f-m detector alone - ± 50 kc deviation

obtained from a Boonton Model 155A signal generator modulated externally from a Hewlett-Packard 200C audio oscillator at 2080 cps. Each audio-signal output was measured with a Hewlett-Packard Model 300A Harmonic-Wave Analyzer tuned in turn to the fundamental audio frequency of each signal. Both carriers were maintained as close to 5250 kc as possible, each being modulated ± 22.5 kc for one set of data (Figure (39)) and ± 50 kc for the other (Figure (40)).

For purposes of analyzing Figure 39, assume that signal D (2080-cps modulation) is the desired signal and signal U (2000-cps modulation) is the undesired signal. The ratio U/D represents the ratio of undesired to desired signal-input levels. It is seen that the capture threshold (3-db depression of D) occurs at U/D = 0 db. Beyond this threshold point, the slope of D reaches 45°. This experimental curve agrees with the previously discussed theoretical results for the case of the linear detector alone with no limiter present. Increased deviation should not appreciably change the capture slope, as is demonstrated in Figure 40.

Figure 41 shows over-all a-m and f-m capture curves as taken with an X-RDZ-2 receiver under two conditions of limiting for the f-m case. An unmodulated carrier was used as the undesired or interfering signal. The desired signal, D, was deviated ± 7.5 kc for FM at 1000 cps, with 100 percent modulation at 1000 cps for the a-m case. The desired-signal input level was maintained constant at 5 microvolts, the input ratio U/D being varied by changing the input level of the undesired unmodulated carrier U only. Both signals were fed to the first detector grid at a carrier frequency of 15.1 Mc. The desired signal was obtained from a Boonton Model 150A signal generator, while the undesired signal was provided from a Measurements Model 65B signal generator. Both the i-f and a-f selectivity controls were in "narrow" position (105 kc and 350-3500 cps bandwidth respectively). The r-f gain control was held constant, with the output level of the desired signal (without interference) being initially adjusted to 6 milliwatts with 5-microvolts input by means of the audio gain control. The AVC was off for all f-m measurements. Output-signal level measurements were made with a Model 300A Hewlett-Packard Wave-Analyzer. The output-noise measurements (modulation off) were made with a Ballantine Model 300 Electronic Voltmeter.

The slope of the "a-m" curve with AVC off (Figure 41) is about 45 to 50°, while with AVC on (Figure 42) it is approximately 60°. These values are in close agreement with the theoretically predicted slopes, (see Figure 23) when receiver saturation effects with AVC off are considered. The "ratio-detector only" curve of Figure 41 has a slope of about 75°, while the "ratio-detector with primary-limiter" curve has a slope of about 78.5°. These

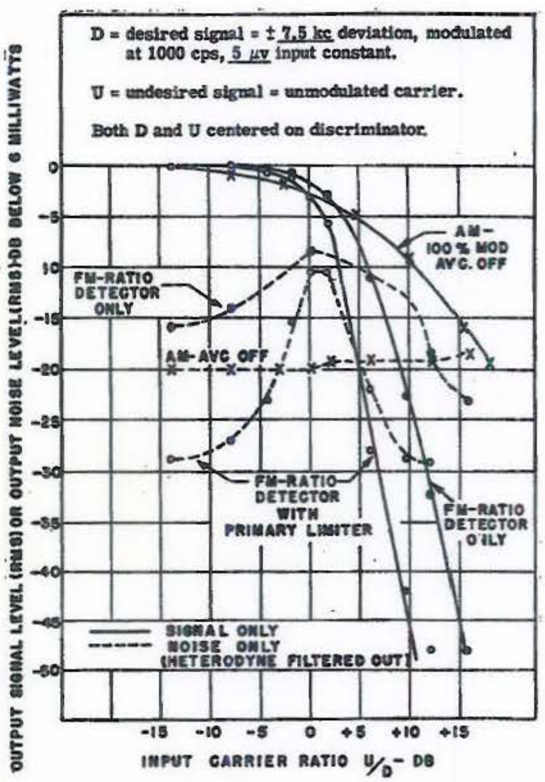

Fig. 41 - Comparison of measured a-m and f-m co-channel capture effects (desired signal depression and noise variation) - desired signal ±7.5 kc deviation for FM, 100 percent modulation with AVC off for AM - 5 μv input level

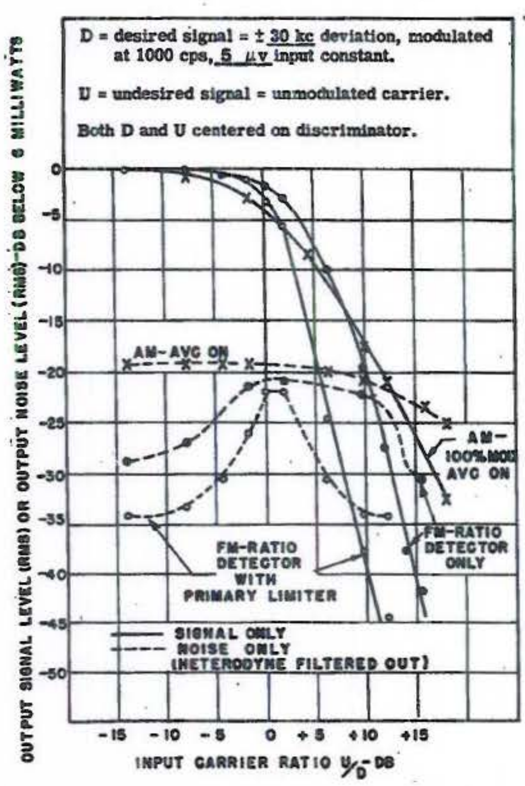

Fig. 42 - Comparison of measured a-m and f-m co-channel capture effects (desired signal depression and noise variation) - desired signal ± 30 kc deviation for FM, 100 percent modulation with AVC on for AM - 5 μv input level

slopes are also in close agreement with the theoretical curves of Figure 23, when the additional limiting, provided by saturation effects in the amplifier stages preceding the f-m detector, is taken into account. The "ratio-detector only" and "ratio-detector with primary-limiter" curves of Figure 42 show slopes which are about the same as those of Figure 41 for the corresponding conditions of operation. The increased deviation used with the f-m signal shows essentially no effect except for some increase in detuning effects.

As shown in Figures 41 and 42, the a-m receiver exhibits little change in output noise with increase of interfering-carrier level, while the f-m receiver shows large noise changes. The f-m noise maximum occurs in the vicinity of input-signal equality (U/D = 1). This noise increase is due to abrupt phase shifts in the resultant of the two carriers, which produces sharp bursts of energy in the output of the f-m detector (see discussion of Figure 6, pages 10 and 11).

The capture curves of Figures 43 and 44 were obtained in a manner similar to that for Figures 41 and 42 except that the input-signal level was increased from 5 to 50 microvolts. The "a-m" curve of Figure 43 (AVC off) has a slope of about 60°. This shows that at high-input levels amplifier saturation preceding the a-m detector produces capture effects similar to those obtained with AVC. The "a-m" curve of Figure 44 (AVC on) also has a capture slope of about 60°, indicating that the maximum capture slope possible in an

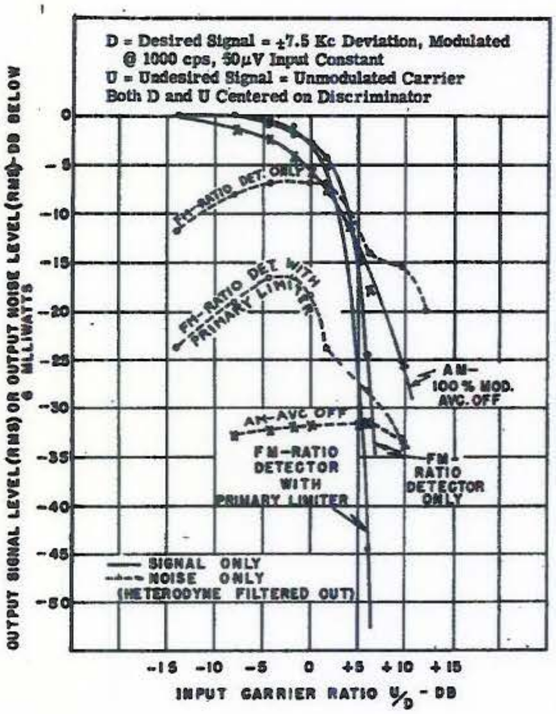

Fig. 43 - Comparison of measured a-m and f-m co-channel capture effects (desired signal depression and noise variation) - desired signal ±7.5 kc deviation for FM, 100 percent modulation with AVC off for AM - 50 μv input level

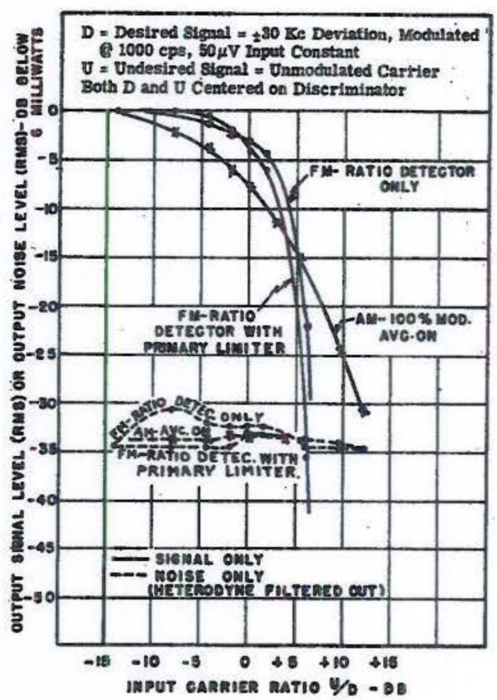

Fig. 44 - Comparison of measured a-m and f-m co-channel capture effects (desired signal depression and noise variation) - desired signal ± 30 kc deviation for FM, 100 percent modulation with AVC on for AM - 50 μv input level

a-m system is in the vicinity of 60° and that this results from the combination of linear detector plus AVC (or amplifier saturation) as previously discussed and shown in Figure 20. The "f-m" curves of Figures 43 and 44 are very similar to those previously shown in Figures 41 and 42.

Impulse Noise

In Figure 45 is shown the effect of impulse noise on the output S/N ratio of the X-RDZ-2 receiver used in previous tests for two conditions of limiting with FM. The impulse-noise source was a Strobotac feeding pulses to the first-detector grid of the receiver at a rate of approximately 200 cps.

It can be seen that strong impulse noise seriously depresses the output S/N ratio. It is also evident, however, that the improvement which the ratio-detector with primary-limiter exhibits over the ratio-detector only on fluctuation noise is maintained quite closely with impulse noise present. At the 5-microvolt input level, for instance, the difference in output S/N ratio between the two with fluctuation noise only is about 11 db, while with impulse noise present it is about 9 db. The capture of the receiver by the desired signal is much less effective with the noise pulses present, as shown by the change in slope of the curves. For instance, the curve for the ratio-detector plus primary-limiter with no external noise present is about 67°. With impulse noise present, it is about 45°. Similar change occurs with the "ratio-detector only" curve. Better limiting results in a greater capture slope whether the interfering signal is fluctuation noise or impulse noise.

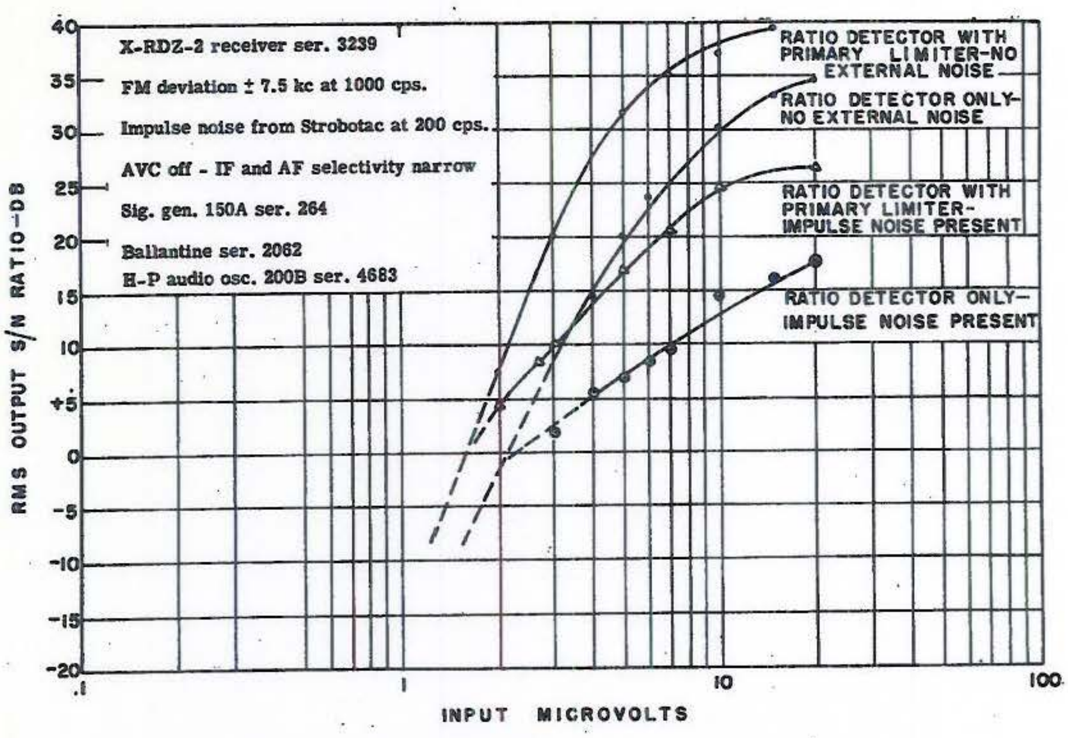

Fig. 45 - Effect on the output S/N characteristics of an f-m receiver of impulse noise under two conditions of limiting

SUMMARY

The "Capture Threshold," as defined in the introduction and used in the discussion, is the undesired-to-desired input carrier level ratio at which the desired-signal output is depressed 3 db below its interference-free value. This has been found, in the experimental data, to be generally in the vicinity of U/D = 1.

The "Standard Depression Capture Ratio," as defined in the introduction, is the undesired-to-desired input carrier level ratio at which the desired-signal output has been depressed to such a degree (30 db) as essentially to prevent transfer of intelligence. The input ratio U/D at which this value of depression is reached depends on the slope of the capture curve and thus on the type of modulation and the circuit characteristics of the particular receiver being examined. For example, in Figure 41, the Standard Depression for the ratio-detector with primary limiter occurs at an input-ratio value of about +7 db, for the ratio-detector only at about +11 db, and for AM with no AVC at about +25 db.

The "Complete Capture Level" is the desired-signal output level at which the desired signal is apparently eliminated completely from the output of the receiver. In general, this level can be taken as approximately 45-50-db depression of the desired signal.

Table 1 summarizes the capture slopes which are obtained under the specified conditions by the listed elements of a receiving system.

Table 2 summarizes the variations in capture slope which are obtained in an f-m system with nonlinearities and nonsymmetries of the discriminator characteristic (input spectrum centered and detuned).

GENERAL DISCUSSION

"Capture" is a desired-signal depression effect which occurs in both a-m and f-m reception. It is generally present whenever an interfering signal stronger than the desired signal is tuned to or near the desired-signal frequency. The resulting depression of the weaker signal by the stronger occurs to a degree which depends on the relative and absolute amplitudes of the two input signals and their frequency separation relative to the limits of the predetector selectivity of the receiver. As defined and treated in this report, the effect is divorced from beat-note and/or various other co-channel and adjacent-channel effects (such as cross-modulation and "swish") that may result in auditory masking in the output. In f-m reception, the effect is caused by the combination of limiter, discriminator and rectifier (detector) action. In a-m reception, the effect is the result of detector and AVC (or predetector saturation) action. The absolute amplitudes of the input signals in conjunction with the thermionic-bias potentials in diodes used as detectors and limiters affects the onset (or threshold) of capture. The degree of capture in an f-m receiver is generally greater than that in a comparable a-m receiver. This difference can be attributed primarily to the influence of the limiter and discriminator circuits in the f-m receiver.

The susceptibility of a receiver to capture can be determined roughly from a plot of input-signal level vs. output signal-to-noise ratio with one-signal input, although not as precisely as with a typical two-signal capture curve. The inherent fluctuation noise of the receiver can be considered as equivalent to the second (undesired) carrier used in the usual capture measurements with, however, the desired-signal input level being varied instead of the undesired-signal input level. The result of improved limiting in a properly aligned f-m receiver, carefully centered on a desired-signal carrier, is an increase in the output S/N ratio, particularly at the medium and higher input levels, and a tendency toward increased capture.

TABLE 1

Condition	Capture Slope		Threshold Depression	
	AM	FM	AM	FM
(1) AM and FM - ideal square-law detector (no limiting)	0°	0°	0 db	3 to 4 db
(2) AM and FM - ideal linear-law detector (no limiting)	45°	45°	3 to 6 db	3 to 6 db
(3) AM and FM - ideal linear-law detector and ideal AVC (no limiting)	63.5°	63.5°	3 to 6 db	3 to 6 db
(4) FM - ideal square-law detector and one-stage ideal limiter (linear and symmetrical discriminator)	---	63.5°	---	3 to 6 db
(5) FM - ideal linear-law detector and one-stage ideal limiter (linear and symmetrical discriminator)	---	71.5°	---	3 to 6 db
(6) FM - ideal linear-law detector and two cascaded ideal limiters (linear and symmetrical discriminator)	---	76°	---	3 to 6 db
(7) FM - maximum possible capture (theoretical)	---	approaching 90°	---	3 to 6 db
(8) FM - typical condition (practical)	---	70 to 80°	---	2 to 4 db
(9) AM - ideal square-law detector and ideal AVC (no limiting)	45°	---	3 to 6 db	---
(10) AM - maximum possible capture (theoretical)	63.5°	---	3 to 6 db	---
(11) AM - typical conditions (practical) no predetector saturation				
AVC on	60°	---	2 to 4 db	---
AVC off	45°	---	2 to 4 db	---

Note: Conditions (1) through (11) in intermediate form (ineffective limiter, detector intermediate between linear-law and square-law, etc.) result in capture slopes generally less than those given for each of the listed conditions of the receiving system. For example, if condition (2) above were to include a detector characteristic intermediate between linear-law and square-law, the capture slope would be intermediate between 0 and 45°.

TABLE 2

Discriminator	Input Spectrum	Variations in Capture
(1) Symmetrical and linear	Detuned from center	No effect on capture as long as spectral components do not exceed discriminator bandwidth.
(2) Nonsymmetrical and nonlinear	Detuned from center	Capture generally less than that listed for condition (4) of Table 1 but may approach it as a maximum as input spectrum is detuned off center. Nonlinearity may aid or oppose degree of capture due to nonsymmetry depending on the curvature of discriminator characteristic.
(3) Nonlinear but symmetrical	Centered	Capture slopes greater or less than for condition (4) of Table 1, depending on the degree and form of nonlinearity.
(4) Nonlinear but symmetrical	Detuned from center	Capture generally a maximum with spectrum centered on characteristic, increasing with detuning on either side. Capture slope may be more or less than for linear discriminator characteristic, depending on curvature of discriminator characteristic.
(5) Nonsymmetrical but linear	Centered	Capture slope less than for condition (4) of Table 1, with actual degree of capture dependent on form of nonsymmetry.
(6) Nonsymmetrical but linear	Detuned from center	Capture a minimum with spectrum in vicinity of center of discriminator characteristic, but increases with detuning on either side of center. Capture never as great as for a symmetrical discriminator characteristic until entire spectrum is to one side of center.

The insertion of a de-emphasis circuit after the final detector of either an a-m or an f-m receiver results in an over-all average output S/N improvement of 1 to 5 db for the f-m system and about 3 to 5 db for the a-m system. These figures are for the particular conditions under which the experimental investigations were conducted. Other figures may be obtained under other conditions of bandwidth, deviation, de-emphasis, and other factors. Addition of de-emphasis has no direct influence on capture.

The effects of detuning at medium- and low-input levels with one-signal input are more severe with an ideal limiter than with a less effective one, i.e., the rate of output S/N deterioration is greater with a nearly-perfect limiter for a given degree of detuning, although the output S/N ratio when accurately centered on the desired-signal carrier is also greater with the more ideal limiter as compared to the imperfect one. This effect is primarily due to unbalance of the noise components in the output of the detector rectifiers. It is interesting to note that a greater deterioration of output S/N ratio with detuning is associated with circuitry which provides greater capture effect. At higher input levels, the output noise is essentially constant with detuning across the selectivity band for all degrees of limiting. Thus at the higher input levels, the detuning curves are virtually independent of limiter characteristics. The effects of detuning on output S/N ratio in an a-m system are negligible within the selectivity limits of the receiver, and capture is likewise virtually unaffected.

It is interesting to note that the so-called overload-selectivity characteristic of an a-m receiver is, in effect, a measure of the frequency separation between desired and undesired signals necessary to reach the capture threshold with various levels of interfering signal. Such a characteristic is usually measured by determining the unmodulated interfering-signal input level required to depress the desired modulated-signal output by 3 db (sometimes 6 db) at various frequency separations. This is, however, not a substitute for a direct co-channel capture measurement.

Capture is an effect largely dependent on relative input-signal amplitudes and is not directly frequency-dependent except insofar as the distribution of frequency selectivity in a receiving system influences the signal amplitudes in the various stages of the receiver. Adjacent-channel capture will differ from co-channel capture mainly in the magnitude of the interfering-signal input levels required to produce the depression effect. Other phenomena, such as control-grid circuit rectification effects, in the early stages of a receiving system with strong interfering-signal input levels may, however, help to obscure the basic capture phenomena in the case of adjacent-channel interference.

CONCLUSIONS

It is concluded that

(a) Capture effects occur in both a-m and f-m receiving systems, differing, however, in degree.

(b) Capture effects are generally greater in an f-m receiving system than in an a-m receiving system.

(c) The difference in degree of capture between a-m and f-m receiving systems can be attributed to the action of the limiter and discriminator circuits in the f-m receiver, which circuits normally do not appear in the a-m receiver.

(d) The more closely the various circuits and stages of an f-m or a-m receiver approach the ideal (ideal limiting, linear discriminator characteristic, and linear-law detectors for FM; linear-law detector and ideal AVC system for AM) the greater the degree of capture.

(e) The susceptibility of a-m systems to capture may be reduced by

(1) The use of square-law rectifiers as final detectors. Such rectifiers are undesirable with double-sideband AM because of their output-distortion

properties but are desirable with single-sideband AM, where their use can result in low output distortion.

(2) Operation without AVC. This is useful only at signal-input levels at which predetector amplifier saturation does not occur. Such saturation can be prevented by careful receiver design and judicious use of manual gain control of the predetector amplifiers, within, however, rather narrow useful limits.

(f) The susceptibility of f-m systems to capture may be reduced by

(1) The use of square-law rectifiers as detectors following the discriminator (slope-filter) element. The opposing or balanced rectifiers generally employed in f-m detector circuits will tend to reduce the output distortion.

(2) Increase in discriminator bandwidth. This decreases the selectivity of the discriminator element between the output of the final r-f (or i-f) amplifier and the detector rectifiers and also decreases detector sensitivity in terms of output volts per cycle (or kilocycle) of deviation. The decrease in selectivity, if important, can be compensated for in circuits preceding the discriminator; and the decrease in detector sensitivity, which is really only a change in transmission gain, can generally be compensated for by an increase in gain elsewhere in the receiver system.

(3) Reduction in effectiveness of limiting. This involves a loss in output signal-to-noise ratio for input-signal levels above the very weak signal region but has the advantage of reducing the S/N ratio loss which results from detuning. It can be accomplished most readily by use of half-wave limiting detectors, such as the ratio-type, and the incorporation of suitable AVC systems which prevent predetector amplifier saturation effects.

(4) Incorporation of discriminators with nonsymmetrical and/or nonlinear characteristics. This is not to be recommended, since these characteristics, in order to be effective, must be such as will result in extreme output distortion.

ACKNOWLEDGMENTS

W. E. W. Howe, who has prepared the forthcoming companion report (NRL Report R-3460) under this problem, was extremely helpful throughout the experimental phases of the work. R. M. Maiden aided greatly in the theoretical analysis, especially in connection with Appendix B. Appreciation is expressed to Emerick Toth for his constant encouragement and leadership and especially for his help in the analysis of data and the examination and derivation of theory.

* * *

APPENDIX A

Depression of a Desired Signal by an Undesired Signal in an A-M Detector with a Linear-Law Detection Characteristic[9]

Let the undesired-signal carrier be $U_i \cos \omega_1 t$ and the desired-signal carrier be $D_i \cos \omega_2 t$. Then the total carrier input to the detector is

$$E_i = U_i \cos \omega_1 t + D_i \cos \omega_2 t$$

$$= U_i \cos \omega_1 t + D_i \cos (\omega_1 + \rho) t$$

where $\rho = (\omega_2 - \omega_1)$ and is assumed to be a supersonic angular frequency. Then,

$$E_i = \sqrt{U_i^2 + D_i^2 + 2U_i D_i \cos \rho t} \cos (\omega_1 t + \phi)$$

where[14]

$$\phi = \tan^{-1} \frac{D_i \sin \rho t}{U_i + D_i \cos \rho t} \quad .$$

We can express the properties of any rectifier in terms of the rectifier-circuit mean current, i, and the peak amplitude, A, of a simple periodic emf (an unmodulated carrier) applied to it. Then, if this relation has no discontinuities,

$$\bar{i} = (\alpha A + \beta A^2 + \gamma A^3 + \delta A^4 + - - -).$$

In a perfectly linear rectifier, $\bar{i} = \alpha A$.

Now let $$T = \sqrt{U_i^2 + D_i^2 + 2U_i D_i \cos \rho t} \quad ,$$

where $\cos(\omega_1 t + \phi) = 1$ for the peak condition of amplitude specified. Simplifying the above expression gives,

$$T = \sqrt{U_i^2 + D_i^2} \left(1 + \frac{2U_i D_i \cos \rho t}{U_i^2 + D_i^2}\right)^{1/2},$$

and putting the above through a binomial expansion gives

$$T = \sqrt{U_i^2 + D_i^2} \left(1 + \frac{U_i D_i \cos \rho t}{U_i^2 + D_i^2} - \frac{1}{2} \frac{U_i^2 + D_i^2 \cos^2 \rho t}{(U_i^2 + D_i^2)^2} + - - -\right).$$

The mean value (integrated over one complete cycle) of the above expression is

$$\bar{T} = \sqrt{U_i^2 + D_i^2} \left(1 - \frac{1}{4} \frac{U_i^2 D_i^2}{(U_i^2 + D_i^2)^2} + - - - -\right),$$

and since $\bar{T} = A$,

$$\bar{i} = \alpha\left(\sqrt{U_i^2 + D_i^2} - \frac{1}{4}\,\frac{U_i^2 D_i^2}{(U_i^2 + D_i^2)^{3/2}} + \cdots\right). \tag{1A}$$

Let the desired signal be amplitude-modulated to $D \pm \Delta D$. Then to find the change of signal current, i, in the presence of the undesired signal, U, we must find $\Delta \bar{i}/\Delta D$ from equation (1A) above. Thus,

$$\frac{\Delta \bar{i}}{\Delta D} = \alpha\left(\frac{D_i}{U_i\left(1 + D_i^2/U_i^2\right)^{1/2}} - \frac{1}{2}\,\frac{D_i}{U_i\left(1 + D_i^2/U_i^2\right)^{3/2}} + \frac{3}{4}\,\frac{D_i^3}{U_i^3\left(1 + D_i^2/U_i^2\right)^{5/2}} - \frac{5}{4}\,\frac{D_i^3}{U_i^3\left(1 + D_i^2/U_i^2\right)^{7/2}} + \cdots\right). \tag{2A}$$

Now let $$x = \frac{U_i}{D_i} = \frac{\text{undesired carrier input amplitude}}{\text{desired carrier input amplitude}},$$

and let $$y = \frac{1}{x} = \frac{D_i}{U_i}.$$

The desired-signal output in the presence of the undesired carrier is represented by $\Delta \bar{i}/\Delta D$, which we will designate D_o. Substituting in equation (2A) gives

$$D_o = \left(\frac{y}{(1 + y^2)^{1/2}} - \frac{1}{2}\,\frac{y}{(1 + y^2)^{3/2}} + \frac{3}{4}\,\frac{y^3}{(1 + y^2)^{5/2}} - \frac{5}{4}\,\frac{y^3}{(1 + y^2)^{7/2}} + \cdots\right). \tag{3A}$$

If it is assumed that $y^2 \ll 1$, then $D_o = y/2$, and thus the modulation of the desired modulated carrier is reduced to a fraction, $D_i/2U_i$, of its original value.

In a similar manner, the influence of the undesired carrier on the desired modulated carrier in the region where $y^2 \gg 1$ may be found. Let $D_o' = \Delta \bar{i}/\Delta D$ in the region where carrier $D_i \gg U_i$. Then,

$$D_o' = 1 - \frac{y^2}{4} = 1 - \frac{1}{4}\left(\frac{D_i}{U_i}\right)^2,$$

or the demodulation influence of the undesired signal on the desired signal is small when the undesired signal is much smaller than the desired signal.

* * *

APPENDIX B

Depression of a Desired Signal by an Undesired Signal in an A-M Detector with a Linear-Law and a Square-Law Detection Characteristic[15]

Let the equation

$$e_i = U \sin (\omega + \rho)\, t + D\,(1 + m \cos \Omega t) \sin \omega t$$

represent the total carrier input to the detector, where D represents the desired modulated signal and U represents the undesired interference consisting of an unmodulated carrier. Then,

$$\begin{aligned} e_i &= U \sin (\omega+\rho)\, t + D \sin \omega t + m\, D \cos \Omega t \sin \omega t \\ &= U \sin (\omega+\rho)\, t + D \sin \omega t + \frac{mD}{2}\left[\sin (\omega+\Omega)\, t + \sin (\omega-\Omega)\, t\right] \\ &= U \sin (\omega+\rho)\, t + D \sin \omega t + \frac{mD}{2} \sin (\omega+\Omega) t + \frac{mD}{2} \sin (\omega-\Omega)\, t. \end{aligned}$$

The envelope of the above expression is given by the summation of the square of the amplitudes, plus two times the sum of the cross-products, times the cosine of the difference in phase angles, or

$$\begin{aligned} (\text{env.})^2 &= U^2 + D^2 + \frac{m^2D^2}{2} + 2\, DU \cos \rho t + mDU \cos (\rho-\Omega)\, t \\ &\quad + mDU \cos (\rho+\Omega)\, t + m D^2 \cos \Omega t + m D^2 \cos \Omega t + \frac{m^2 D^2}{2} \cos 2\,\Omega t \\ &= U^2 + D^2 + 2m\, D^2 \cos \Omega t + m^2 D^2 \cos^2 \Omega t - \frac{m^2 D^2}{2} \\ &\quad + \frac{m^2 D^2}{2} + mDU\, 2 \cos \rho\, t \cos \Omega t + 2\, DU \cos \rho t \\ &= U^2 + D^2\, (1 + m \cos \Omega t)^2 + 2DU\, (1 + m \cos \Omega t) \cos \rho t. \end{aligned}$$

For a square-law detector,

$$\begin{aligned} e_o &= K_2\, (\text{env.})^2 = K_2 \left[U^2 + D^2\, (1 + m \cos \Omega t)^2 + 2DU\, (1 + m \cos \Omega t) \cos \rho\, t\right] \\ &= K_2 \left[U^2 + D^2 + 2mD^2 \cos \Omega t + D^2 m^2 \cos^2 \Omega t + 2DU \cos \rho\, t \right. \\ &\quad \left. + m\, 2\, DU \cos \Omega t \cos \rho t\right] \\ &= K_2 \left[U^2 + D^2 + 2\, mD^2 \cos \Omega t + \frac{D^2 m^2}{2} (1 + \cos\, 2\, \Omega\, t) \right. \\ &\quad \left. + 2\, DU \cos \rho\, t + m\, DU \left\{\cos (\rho+\Omega)\, t + \cos (\rho - \Omega)\, t\right\}\right]. \end{aligned}$$

The modulation output is given by

$$e_o\Big|_{\Omega} = K_2\, 2\, mD^2 \cos\Omega t \qquad (1B)$$

and since the above equation (1B) is independent of U, capture effect does not occur.

For a linear-law detector,

$$e_o = K\,(\text{env.}) = K\left[U^2 + D^2(1 + m\cos\Omega t)^2 + 2DU(1 + m\cos\Omega t)\cos\rho t\right]^{1/2}$$

$$= KU\left[1 + \frac{D^2}{U^2}(1 + m\cos\Omega t)^2 + 2\frac{D}{U}(1 + m\cos\Omega t)\cos\rho t\right]^{1/2}.$$

If we let $\epsilon = \frac{D}{U}$ and $\alpha = 1 + m\cos\Omega t$, then

$$e_o = KU\left[1 + \epsilon^2\alpha^2 + 2\epsilon\alpha\cos\rho t\right]^{1/2}.$$

Expanding the above equation in the binomial form gives

$$e_o = KU\left[1 + \frac{1}{2}(\epsilon^2\alpha^2 + 2\epsilon\alpha\cos\rho t) + \left(\frac{1}{2}\right)\left(-\frac{1}{2}\right)\frac{(\epsilon^2\alpha^2 + 2\epsilon\alpha\cos\rho t)^2}{2}\right.$$

$$+\left(\frac{1}{2}\right)\left(-\frac{1}{2}\right)\frac{\left(-\frac{3}{2}\right)(\epsilon^2\alpha^2 + 2\epsilon\alpha\cos\rho t)^3}{3\cdot 2}$$

$$\left.+\left(\frac{1}{2}\right)\left(-\frac{1}{2}\right)\frac{\left(-\frac{3}{2}\right)\left(-\frac{5}{2}\right)(\epsilon^2\alpha^2 + 2\epsilon\alpha\cos\rho t)^4}{4\cdot 3\cdot 2} + \cdots\cdots\right]$$

$$e_o = KU\left[1 + \frac{\epsilon^2\alpha^2}{2} + \epsilon\alpha\cos\rho t - \frac{1}{8}(\epsilon^4\alpha^4 + 4\epsilon^3\alpha^3\cos\rho t + 4\epsilon^2\alpha^2\cos^2\rho t)\right.$$

$$+\frac{1}{16}(\epsilon^6\alpha^6 + 6\epsilon^5\alpha^5\cos\rho t + 12\epsilon^4\alpha^4\cos^2\rho t + 8\epsilon^3\alpha^3\cos^3\rho t)$$

$$-\frac{5}{128}(\epsilon^8\alpha^8 + 8\epsilon^7\alpha^7\cos\rho t + 24\epsilon^6\alpha^6\cos^2\rho t + 16\epsilon^5\alpha^5\cos^3\rho t$$

$$\left.+ 16\epsilon^4\alpha^4\cos^4\rho t) + \cdots\cdots\right]$$

$$e_o \cong KU\left[1 + \epsilon\alpha\cos\rho t + \frac{\epsilon^2\alpha^2}{2} - \frac{1}{2}\epsilon^2\alpha^2\cos^2\rho t\right].$$

Neglecting terms containing ϵ^n where $n > 2$, since ϵ is a small number (i.e., this applies for all cases where U/D>2),

$$e_o \cong KU \left[1 + \epsilon(1 + m\cos\Omega t)\cos\rho t + \frac{\epsilon^2}{2}(1 + m\cos\Omega t)^2 - \frac{1}{2}(\epsilon^2)(1 + m\cos\Omega t)^2 \cos^2\rho t\right]$$

$$\cong KU \left[1 + \epsilon\cos\rho t + m\epsilon\cos\Omega t\cos\rho t + \frac{\epsilon^2}{2}(1 + 2m\cos\Omega t + m^2\cos^2\Omega t) - \frac{\epsilon^2}{2}(1 + 2m\cos\Omega t + m^2\cos^2\Omega t)\frac{(1+\cos 2\rho t)}{2}\right]$$

$$\cong KU \Big[1 + \epsilon\cos\rho t + \frac{m\epsilon}{2}\cos(\rho + \Omega)t + \frac{m\epsilon}{2}(\cos\rho - \Omega)t$$
$$+ \frac{\epsilon^2}{2} + \frac{2\epsilon^2}{2} m\cos\Omega t + \epsilon^2 m^2 \frac{(1 + \cos 2\Omega t)}{2}$$
$$- \frac{\epsilon^2}{4}(1 + 2m\cos\Omega t + m^2\cos^2\Omega t + \cos 2\rho t$$
$$+ 2m\cos\Omega t\cos 2\rho t + m^2\cos^2\Omega t\cos 2\rho t)\Big]$$

$$e_o \cong KU \Big[1 + \epsilon\cos\rho t + \frac{m\epsilon}{2}\cos(\rho + \Omega)t + \frac{m\epsilon}{2}\cos(\rho - \Omega)t$$
$$+ \frac{\epsilon^2}{2} + \epsilon^2 m\cos\Omega t + \frac{\epsilon^2 m^2}{2} + \frac{\epsilon^2 m^2\cos 2\Omega t}{2} - \frac{\epsilon^2}{4}$$
$$- \frac{\epsilon^2}{2} m\cos\Omega t - \frac{\epsilon^2}{4} m^2 \frac{(1 + \cos 2\Omega t)}{2} - \frac{\epsilon^2}{4}\cos 2\rho t$$
$$- \frac{\epsilon^2}{4} 2m \left\{\cos(2\rho + \Omega)t + \cos(2\rho - \Omega)t\right.$$
$$- \frac{\epsilon^2}{4} m^2 \frac{(1 + \cos 2\Omega t)}{2}\cos 2\rho t\Big]$$

$$\cong KU \Big[1 + \epsilon\cos\rho t + \frac{m\epsilon}{2}\cos(\rho + \Omega)t + \frac{m\epsilon}{2}\cos(\rho - \Omega)t + \frac{\epsilon^2}{2}$$
$$+ \epsilon^2 m\cos\Omega t + \frac{\epsilon^2 m^2}{2} + \frac{\epsilon^2 m^2\cos 2\Omega t}{2} - \frac{\epsilon^2}{4} - \frac{\epsilon^2}{2} m\cos\Omega t$$
$$- \frac{\epsilon^2 m^2}{8} - \frac{\epsilon^2 m^2\cos 2\Omega t}{8} - \frac{\epsilon^2}{4}\cos 2\rho t - \frac{\epsilon^2}{2} m\cos(2\rho + \Omega)t$$

$$-\frac{\epsilon^2 m}{2}\cos(2\rho-\Omega)t-\frac{\epsilon^2 m^2}{8}\cos 2\rho t-\frac{\epsilon^2 m^2}{16}\cos(2\rho-2\Omega)t-\frac{\epsilon^2 m^2}{16}\cos(2\rho+2\Omega)t\Big]$$

$$\cong KU\Big[1+\frac{\epsilon^2}{2}+\frac{\epsilon^2 m^2}{2}-\frac{\epsilon^2}{4}-\frac{\epsilon^2 m^2}{8}+\epsilon\cos\rho t+\frac{m\epsilon}{2}\cos(\rho+\Omega)t$$

$$+\frac{m\epsilon}{2}\cos(\rho-\Omega)t+\left(m\epsilon^2-\frac{m\epsilon^2}{2}\right)\cos\Omega t+\left(\frac{\epsilon^2 m^2}{2}-\frac{\epsilon^2 m^2}{8}\right)\cos 2\Omega t$$

$$-\left(\frac{\epsilon^2}{4}+\frac{\epsilon^2 m^2}{8}\right)\cos 2\rho t-\frac{\epsilon^2}{2}m\cos(2\rho+\Omega)t-\frac{\epsilon^2 m}{2}\cos(2\rho-\Omega)t$$

$$-\frac{\epsilon^2 m^2}{16}\cos(2\rho-2\Omega)t-\frac{\epsilon^2 m^2}{16}\cos(2\rho+2\Omega)t\Big]$$

$$e_0=KU\Big[1+\frac{\epsilon^2}{4}+\frac{3}{8}\epsilon^2 m^2+\epsilon\cos\rho t-\frac{\epsilon^2}{4}\left(1+\frac{m^2}{2}\right)\cos 2\rho t$$

$$-\frac{m\epsilon^2}{2}\cos\Omega t+\frac{3}{8}m^2\epsilon^2\cos 2\Omega t+\frac{m\epsilon}{2}\cos(\rho+\Omega)t+\frac{m\epsilon}{2}\cos(\rho-\Omega)t$$

$$-\frac{\epsilon^2}{2}m\cos(2\rho+\Omega)t-\frac{\epsilon^2 m}{2}\cos(2\rho-\Omega)t-\frac{\epsilon^2 m^2}{16}\cos(2\rho-2\Omega)t$$

$$-\frac{\epsilon^2 m^2}{16}\cos(2\rho+2\Omega)t\Big]\ .$$

The modulation term in the preceding expression is

$$e_0\Big|_{\Omega_2}=K\,\frac{Um\epsilon^2}{2}\cos\Omega t\ . \tag{2B}$$

If the interfering signal, U, were not present, the modulation term would be

$$e_0\Big|_{\Omega_1}=KmD\cos\Omega t. \tag{3B}$$

The ratio of these two expressions is

$$\frac{e_0\Big|_{\Omega_1}}{e_0\Big|_{\Omega_2}}=\frac{KmD\cos\Omega t\,(2)}{KUm\epsilon^2\cos\Omega t}=\frac{2D}{U\epsilon^2}=\frac{2}{\epsilon}=2\,\frac{U}{D}\ . \tag{4B}$$

For all cases where the ratio $U/D > 2$, reduction of output signal in db = $6 + 20\ \log_{10}\frac{U}{D}$ due to presence of U.

* * *

APPENDIX C

Instantaneous Frequency Expression for Resultant, R, of Two Carriers[11]

The simplest case to treat is that of two unmodulated carriers of nearly the same frequency which are added together to produce a heterodyne envelope. This heterodyne results from the beating action of the two voltages producing a variation in the phase of the resultant equivalent to frequency modulation. If the frequency of one carrier is now varied sinusoidally with respect to the other carrier, and if the two carrier amplitudes are kept constant, the result is common or adjacent-channel interference depending on the frequency separation between the two carriers.

Let the desired carrier be represented by

$$D \sin \omega t \qquad (1C)$$

and the undesired carrier by

$$U \sin (\omega + 2\pi\mu)t \qquad (2C)$$

where D = amplitude of the desired carrier,

U = amplitude of the undesired carrier,

ω = angular frequency of desired carrier (radians/sec),

and μ = difference frequency (cycles/sec).

Let $X = U/D$ = input ratio of undesired-to-desired carriers.

If the above signals (equations (1C) and (2C)) are added together, the resultant voltage, E, is

$$(D^2 + U^2 + 2DU \cos 2\pi\mu t)^{1/2} \sin(\omega t + \phi)$$

$$= D(1 + X^2 + 2X \cos 2\pi\mu t)^{1/2} \sin(\omega t + \phi) \qquad (3C)$$

where $\tan\phi = \dfrac{X \sin 2\pi\mu t}{1 + X\cos 2\pi\mu t}$.

The part of equation (3C) contained in the radical represents the heterodyne envelope that would be obtained if the resultant signal was sent through a linear rectifier and the d-c component filtered out.

The two carriers (equations (1C) and (2C)) can be represented vectorially as shown in Figure 46. When t = 0, the two signals are in phase, but since the frequency of D is

Fig. 46 - Vector representation of two carriers

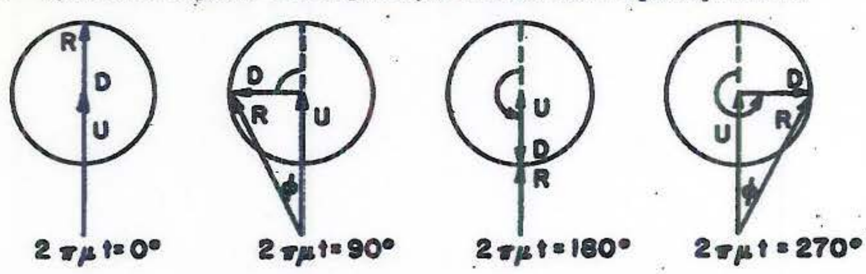

higher than the frequency of U, the vector representing D can be considered as rotating with respect to that representing U. Thus, if U is rotating at ω radians/sec, D will rotate at $\omega + 2\pi\mu$ radians/sec. It is therefore obvious that the phase angle, ϕ, which the resultant R of U and D makes at any given instant with vector U is varying. At time $t = 0, \phi = 0$. When $2\pi\mu t = 90^\circ$, $\tan\phi = D/U = 1/X$. When $2\pi\mu t = 180^\circ$, ϕ is again zero. This rotation of D with respect to U gives the variations in ϕ as shown in Figure 47. The maximum value of ϕ occurs when $\phi = \sin^{-1} 1/X$, as shown in Figure 48. As X approaches unity, ϕ changes more abruptly at values of $2\pi\mu t$ near 180°. When $X = 1$, ϕ increases in a linear fashion from 0° to 90° as D turns through 180° relative to U, as shown in Figure 49. As D approaches cancellation of U, ϕ approaches $+ 90^\circ$, but as D swings past cancellation, the direction of the resultant R suddenly reverses so that $\phi = - 90^\circ$. In other words, there is an instantaneous change in ϕ of 180°.

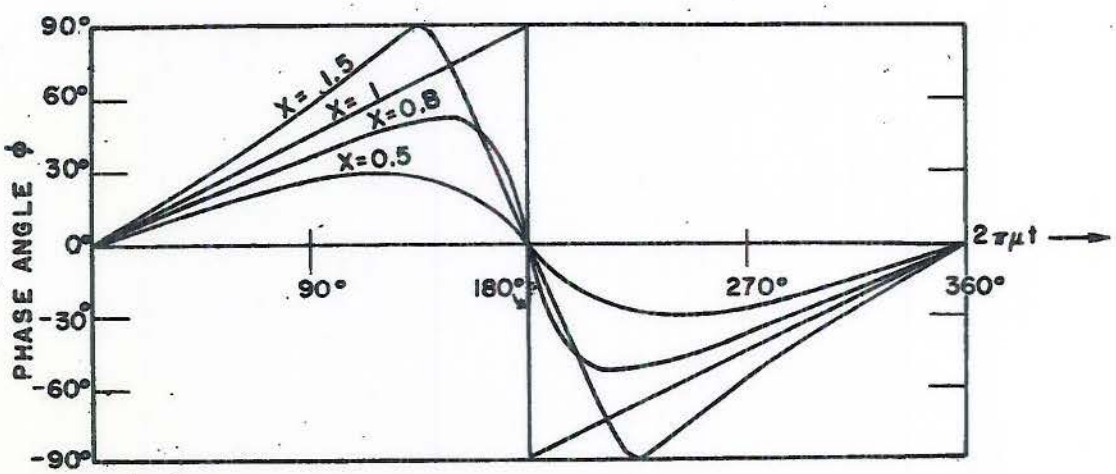

Fig. 47 - Variations in phase angle ϕ for various ratios of X (X = U/D)

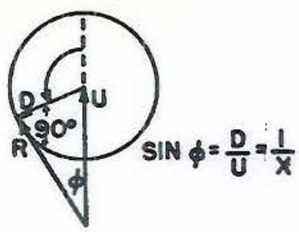

Fig. 48 - Maximum value of phase angle

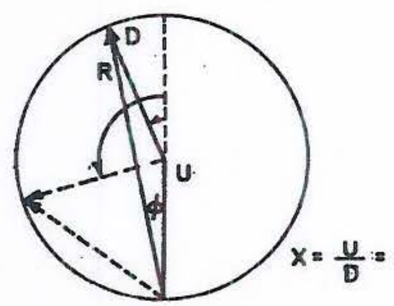

Fig. 49 - Change in ϕ between limits of $2\pi\mu t = 0$ and 180° for the ratio X = 1

The amplitude variations of R in Figure 46, produced by the rotation of D with respect to U, are assumed to be removed by a perfect amplitude limiter. The output resulting from R after limiting and passage through an ideal phase discriminator is then proportional to the slope of the curves of Figure 47, i.e., to the first derivative of ϕ with respect to time. Actual discriminators such as employed in f-m receivers are linear with respect to the frequency displacement or deviation of the resultant whose waveforms may be represented by the time derivatives of the curves of Figure 47. The instantaneous frequency of the resultant, R, is given by

$$f_i = \frac{1}{2\pi}\frac{d}{dt}\text{(argument of sine function, equation (3C))}$$

$$= \frac{1}{2\pi}\frac{d}{dt}(\omega t + \phi)$$

$$= \frac{\omega}{2\pi} + \frac{1}{2\pi}\frac{d}{dt}\tan^{-1}\frac{X\sin 2\pi\mu t}{1 + X\cos 2\pi\mu t}$$

$$= \frac{\omega}{2\pi} + \mu\frac{X\cos 2\pi\mu t + X^2}{1 + X^2 + 2X\cos 2\pi\mu t}$$

or

$$f_i = \frac{\omega}{2\pi} + \left(\frac{\mu}{\dfrac{\cos 2\pi\mu t + 1/X}{\cos 2\pi\mu t + X} + 1}\right), \tag{4C}$$

where the second term (bracketed) represents the frequency deviation resulting from the variation of ϕ.

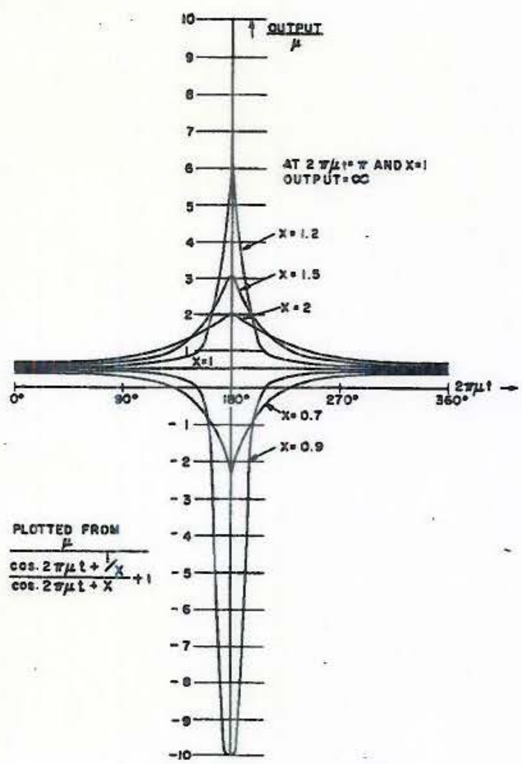

Fig. 50 - Wave-form in audio output for various values of the ratio X

It can be seen from equation (4C) that, as the ratio, X, increases from some value less than unity to values greater than unity, there is an apparent change in the instantaneous frequency, f_i of the resultant approaching μ as a maximum. Figure 50 has been plotted from equation (4C) to show the wave form in the audio output, for various values of X, from an f-m receiver with perfect limiting and a balanced linear detector. As X approaches one, the output becomes more and more like an impulse until, at X = 1, the output has a constant value of 1/2, except that where $2\pi\mu t = \pi$ the output is infinite. When X becomes greater than one, the curves maintain the same relative shape. If the D signal changes position from the high- to the low-frequency side of U signal, then the polarity of the impulses shown in Figure 50 will be reversed.

If one of the two carriers is frequency-modulated, then the beatnote produced in the output of a receiver with a perfect limiter is given by

$$D\cos 2\pi\mu t - \frac{D\cos 2\pi\mu t - \alpha/2\pi}{\dfrac{\cos\beta + 1/X}{\cos\beta + X} + 1} \tag{5C}$$

where

$$\beta = \frac{D}{U} \sin 2\pi\mu t - \alpha t - \theta .$$

Here α is the difference angular frequency and θ is the phase angle which the undesired carrier makes with the desired modulated signal. The two envelopes of maxima and minima of the beat-note pattern are given by

$$\frac{D}{1+X} \cos 2\pi\mu t + \frac{\alpha}{2\pi}\left(\frac{X}{X+1}\right) \tag{6C}$$

and

$$\frac{D}{1-X} \cos 2\pi\mu t + \frac{\alpha}{2\pi}\left(\frac{X}{X-1}\right) \tag{7C}$$

respectively.

* * *

REFERENCES

1. Bureau of Ships Problem Request S1364-A-C of September 10, 1946 entitled "Investigation of Capture Effect in F-M Reception."

2. R.C.A. Patent Disclosure 23343.

3. Ports, D. C, "The AJ Characteristics of F-M Receivers," Jansky and Bailey; NDRC (Div 15), Report OEM sr-1024-24, March 1945. Unclassified.

4. Howe, W. E. W., "An Investigation of Nonlinear Circuits Under Two-Signal Conditions" (Restricted), NRL Report R-3460, to be published.

5. Beatty, R. T., Wireless Eng., 5, 300-303, June 1928.

6. Butterworth, S., Wireless Eng., 6, 619-621, November 1929.

7. Colebrook, F. M., Wireless Eng., 8, 409-412, August 1931.

8. Mallett, E., Wireless Eng., 9, 248-252, May 1932.

9. Appleton, E. V. and Boohariwalla, D., Wireless Eng., 9, 136-139, March 1932.

10. Aiken, C. B., Proc. I. R.E., 19, 120-137, January 1931; 20, 569-578, March 1932.

11. Corrington, M. S., R.C.A. Rev., 7, 522-560, December 1946.

12. Wheeler, H. A., Proc. I. R. E., 28, 537-540, December 1940.

13. Philco Research Division, "Investigation of F-M Detector Circuits," Vol. II, Contract W36-039-SC-32140, July 31, 1947. Restricted.

14. This solution can be found, in slightly different form, in Reich, H. J., "Theory and Application of Electron Tubes," McGraw-Hill, 140-141, 1939.

15. Taken from R. M. Maiden, unpublished data of this Laboratory.

PRNC-709-5-5-49-200